Verification of Model Reduction for Hysteretic Structural Response

by

Ali Mohammed Mirza

Department of Civil and Environmental Engineering
Duke University

Date:_____

Approved:

_____
Henri P. Gavin, Supervisor

_____
Lawrence N. Virgin

_____
Joseph C. Nadeau

Thesis submitted in partial fulfillment of
the requirements for the degree of Master of Science in the Department of
Civil and Environmental Engineering in the Graduate School
of Duke University

2014

ABSTRACT

Verification of Model Reduction for Hysteretic Structural Response

by

Ali Mohammed Mirza

Department of Civil and Environmental Engineering
Duke University

Date:_____

Approved:

_____
Henri P. Gavin, Supervisor

_____
Lawrence N. Virgin

_____
Joseph C. Nadeau

An abstract of a thesis submitted in partial
fulfillment of the requirements for the degree
of Master of Science in the Department of
Civil and Environmental Engineering in the Graduate School of
Duke University

2014

Abstract

The increase in demand for tall and complex structures has increased the need for complex design-oriented analyses for such systems. These analyses involve models with a large number of degrees of freedom and nonlinear (inelastic and geometric) behavior. For seismic design, the Response History Analysis (RHA) is required for base-isolated structures, structures with supplemental damping, and structures located in very high seismic zones RHA on large high-fidelity models is time consuming .Methods to simplify high-fidelity nonlinear models by reducing the number of coordinates involved while maintaining a high degree of modeling accuracy makes RHA less time-consuming and therefore a better design tool. Existing model condensation methods include the Static Condensation Method, Guyan Reduction, and the Dynamic Method. These methods are based on the theory of linearity and superposition, and hence can only be used for linear analysis. Since, all structures do not behave in a linear manner when subjected to severe earthquake loads, it is necessary to compute the seismic responses of structures with inelastic and geometric nonlinearity. There has also been a study in the field of modal superposition that consists of nonlinear time varying modes which is not as accurate as the detailed time-history analysis.

This thesis presents the verification of that meets the need for reduced order modeling of nonlinear structures subjected to earthquake loading. The method uses the dynamic condensation method to reduce the model and then adds hysteretic parameters that can be used to obtain a nonlinear inelastic seismic response. The condensed hysteretic model is then subjected to a set of ground motions and is compared with calculations from the associated high-fidelity model.

Contents

List of Figures

List of Tables

Acknowledgements

Firstly, I would like to take this opportunity to thank Prof. Henri Gavin who served as my advisor throughout my master's program. His nonstop support and guidance made it possible for the completion of this research; I am grateful for his help and look forward to future collaborations in the field of structural dynamics.

I would also like to thank Profs. Lawrence Virgin and Joseph Nadeau for serving on my committee. In addition, I would like to thank Prof. Frank McKenna, OpenSees Expert Developer, for his support in developing a better understanding of OpenSees. OpenSees is a great tool that must be used by every engineer in the field of structural analysis. I would also like to thank Philip Scott Harvey for his time used in explaining me the proposed hysteretic model reduction method.

I would like to take this opportunity to thank my parents – Rafath and Nasreen for their support and love throughout my life. You are the best parents in the world for me, and I will always remember that. My brother and my sisters who have always provided love and continuous encouragement. Finally, I would like to thank my loving wife Sakina, her constant support and love has given me the strength to go through all difficulties that were in front of me.

1. Introduction

The objective of this master's thesis is the verification of a new model reduction method for hysteretic structural systems. Estimation of seismic demands for structures has always been an integral part of structural analysis as it is used for the prediction of life safety and collapse prevention of structures at low performance levels at which the structure is expected to undergo significant inelastic deformations. There have been several procedures to compute seismic demands, amongst them the most widely used by civil engineers are the non-linear response history analysis (RHA), non-linear static procedure (NSP) or pushover analysis in FEMA-273 [1].

The Pushover analysis described in FEMA-273 has been widely used for its simple approach in estimating seismic demands. New methods which involve a lateral load distribution that includes the higher mode effects have been proposed but the result still does not seem to match the seismic demands obtained from a detailed non-linear response analysis [2].

The non-linear response history analysis predicts the forces and deformations demands in every element of the structure by means of a dynamic inelastic analysis using a set of ground motion records, consisting of the one or more components, on the entire structure. The response is calculated taking the behavior of each element into consideration, and thus, is time consuming and rigorous.

The Pushover analysis or the non-linear static procedure (NSP) evaluates the expected performance of a structure by estimating its strength and deformation demands in design earthquakes by means of a static inelastic analysis [2]. The evaluation is based on parameters such as inter-story drift, displacements at nodes, inelastic element deformations as well as the deformations between elements.

Both the above procedures involve the analysis of a detailed and high-fidelity model of the inelastic frame (called the *complete model* in this thesis), this means that the elements are assembled for the entire structure which, upon performing the analysis, results in the computation of nodal displacements at every degrees of freedom. Transient response analysis of such detailed models is time consuming and not practical for early stages of design. Model Condensation is a class of methods by which the complete model can be accurately represented by to a reduced-order model. These reduced models rely on the principles of linearity and superposition, which will be further, discussed in the future chapters. Although the reduction of inelastic frame models cannot invoke superposition, the use of reduced order models in the simulation of complex structural systems would have obvious benefits for the analysis and design of complex inelastic structures.

This thesis first addresses the various model condensation methods that have been developed to date, along with their shortcomings, and will also describe a new model reduction method for hysteretic structural systems. A verification of this new

method will be demonstrated to show that the proposed model reduction can be used to simulate inelastic responses.

In these simulations, the condensed hysteretic model is subjected to a set of earthquake ground motions; its inelastic behavior is observed and compared to a responses computed from the detailed model. The error between the detailed and the condensed model for different seismic demands such as the peak inter-story drift ratio, peak floor accelerations and peak horizontal floor displacements was also checked to verify the use of this proposed model reduction method.

2. Types of Model Condensation

2.1 Static Condensation and Guyan Condensation

The static condensation method involves a coordinate transformation on the stiffness matrix of the detailed structure in order to compute a smaller stiffness matrix for a subset of coordinates, the primary coordinates. Implicit in this transformation is the assumption the secondary coordinates (those eliminated through the coordinate transformation) carry no external forces, and that the displacements of those coordinates are of no interest. The secondary coordinates can be considered as dependent upon the displacements of the primary coordinates, and are therefore expressed in terms of the remaining independent or primary degrees of freedom [3]. The word 'static' has been used as the static relation between the secondary and primary degrees of freedom is the key factor for the reduction of the stiffness matrix. It is also used in static problems to eliminate the internal degrees of freedom of an element used with the Finite Element Method.

Let us assume that the secondary degrees of freedom are to be eliminated or reduced and are arranged as the first s coordinates, whereas the primary (remaining) degrees of freedom are the last p coordinates. Thus, the stiffness equation for the full model can be partitioned as

$$\begin{bmatrix} [K_{ss}] & [K_{sp}] \\ [K_{ps}] & [K_{pp}] \end{bmatrix} \begin{Bmatrix} \{y_s\} \\ \{y_p\} \end{Bmatrix} = \begin{Bmatrix} \{0\} \\ \{F_p\} \end{Bmatrix} \tag{1}$$

Where $\{y_s\}$ is the displacement vector corresponding to s degrees of freedom that will be condensed and $\{y_p\}$ is the vector corresponding to the remaining p degrees of freedom. The reduced stiffness matrix can then be expressed as a transformation of the full model stiffness matrix as follows:

$$[\tilde{T}] = -[K_{ss}]^{-1}\,[K_{sp}] \tag{2}$$

$$[\tilde{T}] = \begin{bmatrix} [\bar{\tilde{T}}] \\ [I] \end{bmatrix} \tag{3}$$

$$[\bar{K}] = [\tilde{T}]^T\,[K]\,[\tilde{T}] \tag{4}$$

Where $[\bar{K}]$ is the reduced stiffness matrix, $[K]$ is the full model stiffness matrix, $[\tilde{T}]$ is the transformation matrix and $[I]$ is the identity matrix.

In Guyan condensation [5] the mass matrix of the full system is reduced by applying the coordinate transformation of the static condensation formula to the mass matrix

$$[\bar{M}] = [\tilde{T}]^T\,[M]\,[\tilde{T}] \tag{5}$$

where $[\bar{M}]$ is the reduced mass matrix and $[M]$ is the full model mass matrix

For models reduced by Guyan Condensation, Kinetic Energy and Potential Energy of the reduced model and full model match whereas; the natural frequencies and mode shapes do not. This use of a static relation between the primary and the secondary degrees of freedom can produce large errors when applied to dynamic problems in which many modes contribute to the response. Thus, an improved method for model condensation of dynamic problems was investigated.

2.2 Dynamic Condensation

An extension to the Guyan Condensation Method for dynamic problems was first introduced by Mario Paz [4] [5]. This method uses the eigenvalue problem of a structural system which consists of the desired reduced secondary degrees of freedom $\{y_s\}$ and the retained primary degrees of freedom$\{y_p\}$. The equation of motion can then be written as

$$\begin{bmatrix}[M_{ss}] & [M_{sp}]\\ [M_{ps}] & [M_{pp}]\end{bmatrix}\begin{Bmatrix}\{\ddot{y}_s\}\\ \{\ddot{y}_p\}\end{Bmatrix}+\begin{bmatrix}[K_{ss}] & [K_{sp}]\\ [K_{ps}] & [K_{pp}]\end{bmatrix}\begin{Bmatrix}\{y_s\}\\ \{y_p\}\end{Bmatrix}=\begin{Bmatrix}\{0\}\\ \{0\}\end{Bmatrix} \tag{6}$$

Substituting $\{y\} = \{Y\}\sin\omega_i\, t$ in the above equation (6) results in the following

$$\begin{bmatrix}[K_{ss}]-\omega_i{}^2[M_{ss}] & [K_{sp}]-\omega_i{}^2[M_{sp}]\\ [K_{ps}]-\omega_i{}^2[M_{ps}] & [K_{pp}]-\omega_i{}^2[M_{pp}]\end{bmatrix}\begin{Bmatrix}\{Y_s\}\\ \{Y_p\}\end{Bmatrix}=\begin{Bmatrix}\{0\}\\ \{0\}\end{Bmatrix} \tag{7}$$

The reduced stiffness matrix can then be expressed as a transformation of the full model stiffness matrix as follows:

$$[T]=\begin{bmatrix}[I]\\ -[K_{ss}-\omega_i{}^2M_{ss}]^{-1}\,[K_{sp}-\omega_i{}^2M_{sp}]\end{bmatrix} \tag{8}$$

$$[\bar{K}]=[T]^T\,[K]\,[T] \tag{9}$$

$$[\bar{M}]=[T]^T\,[M]\,[T] \tag{10}$$

where [T] is the transformation matrix, ω_i is the natural frequency of the i^{th} mode, $[\bar{K}]$ and $[\bar{M}]$ are the reduced stiffness and mass matrix respectively.

The eigenvalue of the reduced stiffness and mass matrix exactly match the eigenvalue of the stiffness and mass matrix of the full model at frequency ω_i and thus can be used for dynamic analysis for responses dominated by modes around the ith

mode. The Static Condensation method, the Guyan Condensation Method, and the Dynamic Condensation method all represent full model coordinates as a linear combination of reduced model coordinates and therefore rely on the principles of linearity and Superposition. Linear behavior can be best described by the following relation:

$$a * y_1 + b * y_2 = f(a * u_1\ b * u_2)$$

$$where, y_1 = f(u_1)\ and\ y_2 = f(u_2)$$

For systems in which responses extend into the inelastic range, superposition does not hold. The model reduction of inelastic structures is therefore a challenging problem.

3. Challenges

3.1 Inelastic response simulations are time consuming

The present method of inelastic response widely used is the nonlinear response analysis. This non-linear response history analysis (RHA) predicts the forces and deformations demands in every element of the structure by means of a dynamic inelastic analysis using a set of ground motion records. The RHA is the most accurate method of calculating the inelastic response of the structure under seismic loads. The response is calculated taking the behavior of each element into consideration, and thus, is time consuming and rigorous.

3.2 Response History Analysis (RHA), Response Spectrum Analysis (RSA) and the Modal Pushover Analysis (MPA)

The Response Spectrum Analysis (RSA) is another procedure which is implemented in a variety of commercial software, is also used to estimate the inelastic behavior of structures under seismic loads. The RSA uses an approximation method in calculating the modal combination of the peak modal responses to estimate the total response. The error in the RSA is similar to the error obtained from the Modal Pushover Analysis when seismic demands are calculated [7]. Due to the presence of this large error when compared with RHA, it is difficult to use the RSA method for important structures with high seismic demands.

The Modal Pushover Analysis was introduced to improve the Pushover Analysis described in FEMA-273. The issue with regards to the calculation of the seismic

demands of the structure using a pushover analysis was thoroughly checked and the errors have been made public in the past [7]. The different lateral load distribution patterns were also checked in order to obtain a better response, but they all seem to have a large error when compare to the RHA. Modal Pushover Analysis is an improved pushover analysis procedure that uses the inertia force distribution for each mode to calculate the seismic demands. The seismic demands for the calculated modes are then combined to provide an estimate of the total seismic demand on inelastic systems.

Unlike the standard pushover analysis where the force distribution and target displacement are based on the assumption that the response is controlled by the fundamental mode remains unchanged even after the structure yields; the MPA uses a combination of higher modes for the redistribution of inertia forces due to structural yielding.

For the elastic multistory structure, the peak response due to its n_{th} vibration mode is determined by subjecting the structure lateral forces distributed over the height of the building according to $s_n^* = m\phi_n$, where m is the mass matrix and ϕ_n is the nth-mode, and the structure is pushed to the roof displacement determined from the peak deformation D_n of the nth-mode elastic SDF system; D_n is available from the elastic response spectrum. Combining these peak modal responses by an appropriate modal combination rule gives the resultant seismic demand.

For inelastic systems, the seismic demands are calculated in two phases. First, a pushover analysis is used to determine the peak response r_{no} of the inelastic MDF system to individual terms $p_{eff,n}(t) = -s_n \ddot{u}_g(t)$, in the modal expansion of the effective earthquakes forces $p_{eff,n}(t) = -m\iota\ddot{u}_g(t)$. The base shear–roof displacement ($V_{bn} - u_{rn}$) curve is developed from a pushover analysis for the force distribution $s_n{}^*$. This pushover curve is idealized as a bilinear force – deformation relation for *n*th-mode inelastic SDF system and the peak deformation of this SDF system (determined by nonlinear response history analysis (RHA) or from the inelastic response or design spectrum) is used to determine the target value of roof displacement at which the seismic response r_{no} is determined by the pushover analysis. Second, the total demand r_o is determined by combining the r_{no} (n=1, 2 …) according to an appropriate modal combination rule (e.g. SRSS rule).

During an elastic analysis, the relative error in the inter-story drift between the RHA and the Modal Pushover Analysis was observed to be the same as the difference seen when implementing the RSA method [7] [8]. It was observed that the RSA method underestimated the elastic response (in terms of inter-story drift) by 15% to 30%. The error in MPA was essentially the same as in RSA.

The above errors discussed in case of MPA or RSA when compared to RHA seem to be extremely large for an elastic response. These methods result in greater errors when the structural response moves into the inelastic range. Another important point to

be noted is that the total response is estimated by combining the peak modal responses using the SRSS rule [9]. The number of modes to be selected is based on the accuracy required. In most cases, three modes are used, but the error is relatively large when compared with the seismic demands obtained from RHA. This means that in order to get a fairly accurate estimation, it is important to condense the model and use the recommended RHA to obtain seismic demands of a structure.

Every structure will behave with nonlinearity if forced strongly enough. The Principle of superposition is applicable only to purely linear systems and is by definition, not possible in a non-linear system.

In linear systems, both the static and dynamic behaviors of a structure are described by models for which static and dynamic solutions are unique. Such models fail to work if the structure goes beyond the linear response range for any reason. A nonlinear model however, describes both the static and dynamical behaviors. This, of course causes a solution which is not unique because of the presence of possibility of several dynamic equilibria coexisting. The one being observed at any time depends on the static equilibria, system parameters, initial conditions, and the trajectory of the states over time.

3.3 Modal superposition technique and its inherent linear assumption

The exact solution for an undamped free vibration problem is usually obtained by substituting the equation into the equation of motion [9]

$$y(t) = \sum_m (A_i \cos \omega_i t + B_i \sin \omega_i t)\ \phi^{(i)}$$

Where "$\phi^{(i)}$" is a modal vector. For the solution, the coefficients A and B are determined from the initial conditions. This method though simple for smaller scale structures, tends to become complicated and impractical as the scale of the structure increases because two coefficients need to be introduced for every mode shape.

In order to solve such a system, we use a technique called Modal Superposition which can be applied to both free and forced vibration systems. In this technique, We first use the free vibration mode shapes of the structure to uncouple the Equations of Motion. These uncoupled equations are now in terms of new variables called modal coordinates. The solution for the modal coordinates can be obtained by solving each equation independently

Finally, superposition of the modal coordinates results in the solution of the original equation. It is not, however necessary to use all possible mode shapes to solve a given problem. Using the first few fundamental modes usually leads to acceptable results. This is evident when we consider the basic formulation of the equations used for

modal superposition. The basic equation of motion of an undamped multi degree of freedom system is given by

$$m\,\ddot{y}(t) + k\,y(t) = f(t);\quad y(0) = u^0\ and\ \dot{y}(0) = v^0$$

For formulating the Model Superposition, we use the equation:

$$y(t) = z_1(t)\phi_1 + z_2(t)\phi_2 + \cdots + z_n(t)\phi_n$$

where the displacement is written as a linear sum of the mode shape vectors.

It is clear from the above solution that the assumption of linear dynamic behavior is inherent in the process of modal superposition. Therefore, a modal superposition cannot be used when we need to model a structure for nonlinear behavior.

3.4 Bouc-Wen hysteretic equation

Hysteresis can be defined as the dependence of any system on not just its current state but the history of its previous states as well. Hysteresis in structures is a natural mechanism that supplies restoring forces against movements and dissipates energy. In other words, Hysteresis in structural components is a reference to the memory nature of inelastic behavior where the restoring force depends not only on the instantaneous deformation but also on the history of deformation [9][10].

The Bouc-Wen hysteresis model is able to capture, in analytical form, a range of hysteretic cycle shapes matching the behavior of a wide class of hysteretic systems [10] [11].

Its basic equation is given as:

$$F(t) = \kappa k_i u(t) + (1 - \kappa) k_i z(t)$$

Where *F (t)* is the restoring force and *z (t)* is a non-observable hysteretic parameter (usually called the hysteretic displacement) that obeys the following nonlinear differential equation with zero initial condition ($z(0) = 0$), and that has dimensions of length.

$$\dot{z}(t) = A\,\dot{u}(t) - \beta\,|\dot{u}(t)||z(t)|^{n-1}\,z(t) - \gamma\,\dot{u}(t)|z(t)|^{n}$$

The restoring force $F(t)$ is decomposed into and elastic part $F^{(el)}$ and a hysteresis part from which, the hysteresis part$F^{(h)}$, which can be integrated to give the dissipated hysteresis energy. This absorbed hysteresis energy represents the energy dissipated by the hysteretic system and is given as the power of the hysteretic force, integrated over time.

$$\varepsilon\,(t) = (1 - \kappa)\omega^2 \int_0^t z(\tau)\dot{u}(\tau)d\tau$$

In the proposed model reduction method, hysteretic behavior is simulated using the following parameters:

- z_{yield} – The yield displacement of the reduced model for each remaining node is used to determine the elastic-plastic behavior of the structure and ranges from 1.2 to 2.5
- κ –is used to describe the post yielding to pre yielding stiffness ratio and ranges from 0.02 to 20.0
- η –is the exponent used to describe the hysteretic knee sharpness and ranges from 3 to 12
- ρ –describes the hysteretic shape factor and ranges from 0 to 1

The number of hysteretic parameters used can vary a minimum of 4 for the entire structure to a maximum of one for each node bringing the total to 13. The values of z_{yield} has been used for each node as inelastic nonlinear response is going to be a check for the entire structure when compared to the detailed model.

3.5 High Fidelity Model and Fiber Elements

A high fidelity model is by definition a model that produces results that are very close or almost identical to those of the actual structure.

The high fidelity models of hysteretic structures used in this research make use of fiber-element discretization of structural frame elements [27]. A fiber element is a structural element that is flexibility-based and is commonly used for nonlinear analysis of hysteretic structures. In OpenSees, the fiber elements are created on the form of a refined grid to numerically evaluate integrals over the cross-sections. The creation of fiber elements helps representing partial yielding and cracking of the cross-section in an accurate manner. [28]

This approach is particularly advantageous when the commonly adopted assumption of uniaxial stress state at the material points of the cross-section is made. Strain-hardening laws with different loading and unloading patterns, and residual stresses are considered with this approach. Creating fiber elements helps distribute the plasticity along the element which uses "Plastic zone" methods that involve numerical integration over the element length.

Using the Gauss-Lobatto quadrature rule, the sections are subdivided into regions of regular shapes over which the numerical integration schemes are employed. This discretization can then be used to calculate the Axial forces and Bending moment over the fiber section. The basic strategy is to divide the element into longitudinal sections or fibers. The geometric properties of the fiber define it, i.e. its location and its cross sectional area. The element fibers follow a uniaxial stress strain relation depending on the material that is being used and this relationship is integrated to a relationship for the section. These elements have their limitations in that the displacements and deformations have to be relatively small and the assumption that plane sections always remain plane [27].

When these elements are to be used, there are two main tasks to be accomplished:

- To determine the state of the element i.e. determining the resisting forces for a given displacement
- Determination of the section flexibility which is then used to determine the element flexibility

The main assumption in a flexibility based model is the internal force distribution which is expressed using force interpolation functions. This process is followed by the computation of fiber stresses based on equilibrium.

The high-fidelity models used in this research make use of the OpenSees computational framework. This framework facilitates nonlinear analyses of structures with inelastic and geometric nonlinearities subjected to earthquake loading. [12]

4. Model Reduction for Hysteretic Structural Behavior

The steps involved in validating the proposed numerical method for model reduction are outlined in this section.

4.1 Step 1: Build a high-fidelity model using fiber-elements and a linear-elastic reduced model of the structural frame.

Brief Description of the High-Fidelity 2D frame model generated in OpenSees

A 2D model for an inelastic frame was in OpenSees [12]. The frame modeled was the subject of previous investigations of pushover analyses [29]. The material properties assigned to each element were defined such that the yield stress of steel was assumed to be 60 ksi, the young's modulus of steel was assumed as 29000 ksi and to define the uniaxial hardening material, the isometric hardening modulus of 0 and kinematic hardening of 10 were assumed. These hardening parameters help explain the plastic behavior of the beam column elements on yielding. Kinematic and isotropic hardening is used based on the characteristic material's yield surface while loading and unloading. In kinematic hardening, initial yield surface translates from the original position, keeping the size of yield surface remains constant. In isotropic hardening, initial yield surface expands from the original position, and the size of the yield surface keeps expanding and growing, typically plastic or hyper-elastic materials come under this category.

The structural layout of the building in figure 1 represents a three-bay five story moment resisting frame with each bay spaced at 20 feet. The first four stories are equally

spaced at 13 feet and the top story has a length of 14 feet. The column elements are the same for the entire frame, W14x145 for all the columns, while the beam sizes vary from floor to floor. The beams present in the second and third floor were modeled using W24x76 section, the beams present in the fourth floor were modeled using W24x68 section and the top floor was modeled using W18x40.

The beam-column elements that were chosen for this model have a flexibility-based formulation in which the distribution of internal forces satisfy equilibrium exactly, strains and curvatures are computed from the internal forces through the fiber-element discretization of the cross section, and these strains and curvatures are integrated to the nodal displacements of the element using numerical integration. The integration points are based upon the Gauss-Lobatto quadrature rule which states that two integration points are present at the element ends [12].

Beam-column elements are discretized into fiber elements which discretize the section into sub regions of simpler, regular shapes (e.g. quadrilateral, circular and triangular regions) called patches. For the selected model we have used the Quad patch, which is used to construct a Patch object with a quadrilateral shape. The geometry of the patch is defined by four vertices. . The fiber elements are associated with models for uniaxial material behavior. Deformations of the fibers enforce the Bernoulli beam assumption which states that a plane section remains plane [12]. For stresses that exceed yield, the strain hardening material that has been defined is used. Pushover responses

were compared for models with different numbers of fiber elements and different numbers of integration points. Static pushover analyses were done on the frame for various integration points ranging from 2 to 10 per element. It was observed that the computed nodal displacements was sensitive to the the number of integration points used to model each element for elements with 2 to 6 integration points. The response was not sensitive to the number of integration points in the range of 7 to 10 integration points per element. To maintain high accuracy throughout the procedure, 10 integration points were selected across the element.

Furthermore, changes in the number of fiber elements used for each section did not have an effect on the computed displacements. Figure 2 and Figure 3 represent the changes observed with the variation of Gauss integration points and the number of fiber elements used.

Figure 1: The 2D Frame selected showing the various beam-column sections and the different spans

The beam column elements were then assigned to the connection of nodes and recorders were defined to obtain the results after the completion of the analysis. The horizontal responses of nodes 21, 31, 41, and 51 are used as the basis of comparison of the various models investigated in this thesis.

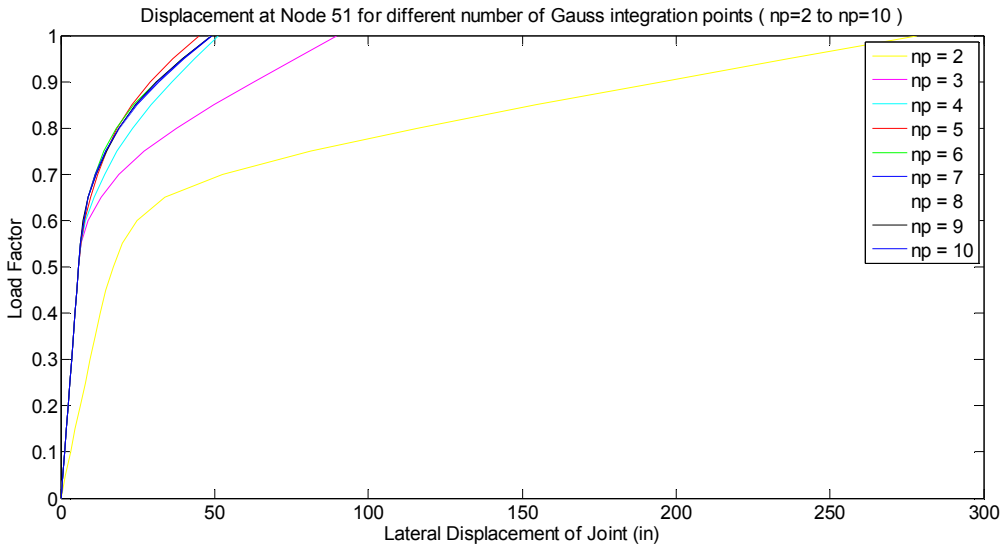

Figure 2: Pushover curve obtained for different number of Gauss integration points.

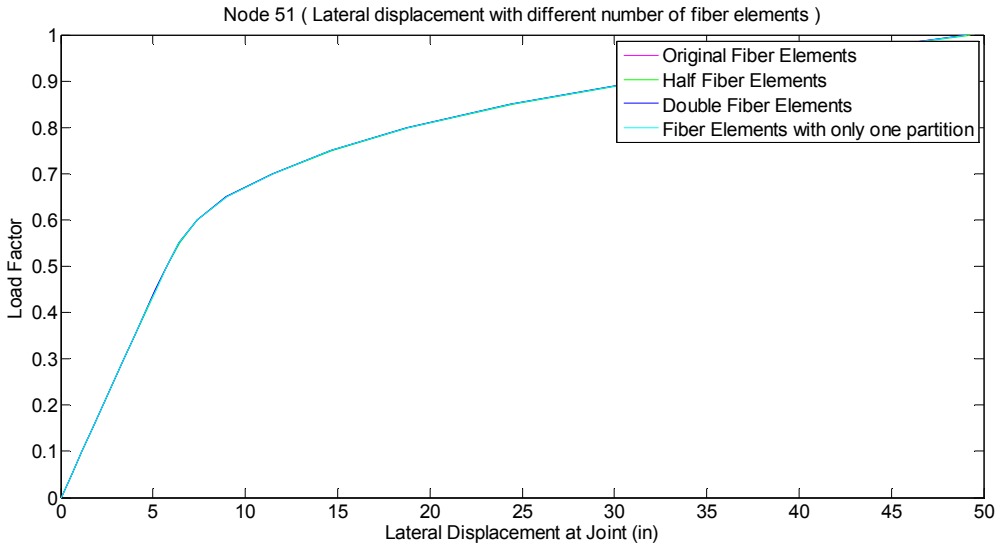

Figure 3: Pushover curve obtained for the different number of fiber elements used.

Linear Elastic Frame Model

A linear elastic frame model was created using the same elastic modulus and element section specification used in the detailed model. Extended Rayleigh damping of 2% in each mode was used during the dynamic analysis. The beams and columns were modeled as 2D frame elements and structural stiffness and mass matrices were assembled from a linear elastic condensed model of the structural frame was obtained using the Dynamic Guyan Condensation. The condensed model reduced the model from 60 coordinates to only 4: the horizontal displacements of nodes 21, 31, 41, and 51. In the dynamic condensation, the selected frequency was the structure's fundamental frequency.

4.2 Step 2: Replacing the linear-elastic restoring force with hysteretic restoring force and introducing the hysteretic displacement variable

Here, we will only continue by using the condensed mass and stiffness matrix obtained by this method of dynamic condensation.

$$\widetilde{\boldsymbol{M}} = \widetilde{\boldsymbol{T}}^{\boldsymbol{T}} \begin{bmatrix} \boldsymbol{M_{pp}} & \boldsymbol{M_{ps}} \\ \boldsymbol{M_{sp}} & \boldsymbol{M_{ss}} \end{bmatrix} \widetilde{\boldsymbol{T}} \tag{11}$$

$$\widetilde{\boldsymbol{K}} = \widetilde{\boldsymbol{T}}^{\boldsymbol{T}} \begin{bmatrix} \boldsymbol{K_{pp}} & \boldsymbol{K_{ps}} \\ \boldsymbol{K_{sp}} & \boldsymbol{K_{ss}} \end{bmatrix} \widetilde{\boldsymbol{T}} \tag{12}$$

$$\tilde{\mu} = \widetilde{\boldsymbol{T}}^{\boldsymbol{T}} \begin{bmatrix} \boldsymbol{M_{pp}} & \boldsymbol{M_{ps}} \\ \boldsymbol{M_{sp}} & \boldsymbol{M_{ss}} \end{bmatrix} \begin{bmatrix} \boldsymbol{J_p} \\ \boldsymbol{J_s} \end{bmatrix} \tag{13}$$

Where, $\widetilde{\boldsymbol{M}}$ is the reduced mass matrix of the condensed system, $\widetilde{\boldsymbol{K}}$ is the reduced stiffness matrix of the condensed system, $\widetilde{\boldsymbol{T}}$ is the condensation transformation matrix.

This reduction reduces the total number of degrees of freedom from the initial value of 60 to 4. The condensed equations of motion are then given as

$$\widetilde{\boldsymbol{M}}\ddot{\boldsymbol{x}} + \widetilde{\boldsymbol{C}}\dot{\boldsymbol{x}} + \widetilde{\boldsymbol{K}}\boldsymbol{x} = -\tilde{\boldsymbol{\mu}}\ddot{\boldsymbol{u}}_{\boldsymbol{g}} \tag{14}$$

Since, we are using the ground motion only in the x direction. The equation of motion can be expressed as

$$\widetilde{\boldsymbol{M}}\ddot{\boldsymbol{x}} + \widetilde{\boldsymbol{C}}\dot{\boldsymbol{x}} + \widetilde{\boldsymbol{K}}\boldsymbol{x} = -\tilde{\boldsymbol{\mu}}\ddot{\boldsymbol{u}}_{\boldsymbol{gx}} \tag{15}$$

Hysteretic Parameters

The reduced structural model is now coupled with a hysteresis model. The following steps are involved in the coupling of the hysteretic model to the condensed linear model. The lower triangular matrix '**T**' relates the horizontal floor displacements with respect to the ground, $\boldsymbol{x}$, to the relative inter-story displacements, denoted by $\boldsymbol{u} = [\boldsymbol{u_1}, \boldsymbol{u_2}, \dots, \boldsymbol{u_n}]$

$$\boldsymbol{T} = \begin{bmatrix} \mathbf{1} & \mathbf{0} & \mathbf{0} & \mathbf{0} \\ \mathbf{1} & \mathbf{1} & \mathbf{0} & \mathbf{0} \\ \mathbf{1} & \mathbf{1} & \mathbf{1} & \mathbf{0} \\ \mathbf{1} & \mathbf{1} & \mathbf{1} & \mathbf{1} \end{bmatrix} \tag{16}$$

$$\boldsymbol{x} = \boldsymbol{T}\boldsymbol{u} \implies \boldsymbol{u} = \boldsymbol{T}^{-\mathbf{1}} \tag{17}$$

This transforms Equation (5) to the relative coordinates,

$$\widetilde{\boldsymbol{M}_{\boldsymbol{u}}}\ddot{\boldsymbol{u}} + \widetilde{\boldsymbol{C}_{\boldsymbol{u}}}\dot{\boldsymbol{u}} + \widetilde{\boldsymbol{K}_{\boldsymbol{u}}}\boldsymbol{u} = -\tilde{\boldsymbol{\mu}}\ddot{\boldsymbol{u}}_{\boldsymbol{gx}} \tag{18}$$

$$\widetilde{\boldsymbol{M}_{\boldsymbol{u}}} = \boldsymbol{T}^{\boldsymbol{T}}[\widetilde{\boldsymbol{M}}]\,\boldsymbol{T} \tag{19}$$

$$\widetilde{\boldsymbol{C_u}} = \boldsymbol{T^T}[\widetilde{\boldsymbol{C}}]\,\boldsymbol{T} \tag{20}$$

$$\widetilde{\boldsymbol{K_u}} = \boldsymbol{T^T}[\widetilde{\boldsymbol{K}}]\,\boldsymbol{T} \tag{21}$$

$$\widetilde{\boldsymbol{\mu_u}} = \boldsymbol{T^T}\widetilde{\boldsymbol{\mu}} \tag{22}$$

The elastic inter-story restoring forces $\boldsymbol{K_u}$are now replaced by hysteretic inter-story shear forces using the following substitution:

$$\widetilde{\boldsymbol{K_u}}\boldsymbol{u} \;\rightarrow\; \boldsymbol{\kappa}\widetilde{\boldsymbol{K_u}}\boldsymbol{u} + (\boldsymbol{1}-\boldsymbol{\kappa})\widetilde{\boldsymbol{K_u}}\boldsymbol{z} \tag{23}$$

Here, κ is the ratio of the post-yield stiffness to the pre-yield stiffness. The auxillary variable $\boldsymbol{z} = [\,\boldsymbol{z_1}, \boldsymbol{z_2}, \ldots, \boldsymbol{z_n}\,]^{\boldsymbol{T}}$ is the isotropic hysteretic displacement which is obtained from the generalized Park-Wen model [10] [11]

$$\dot{\boldsymbol{z}} = \dot{\boldsymbol{u}} - \boldsymbol{z} \circ \boldsymbol{\iota} \tag{24}$$

$$\boldsymbol{\iota} = \{\boldsymbol{\beta} \circ \boldsymbol{abs}(\dot{\boldsymbol{u}} \circ \boldsymbol{z}) - \boldsymbol{\gamma} \circ \dot{\boldsymbol{u}} \circ \boldsymbol{z}\} \circ (\boldsymbol{z} \circ \boldsymbol{z})^{\frac{\eta-2}{2}} \tag{25}$$

Here, the operator 'o' is the element wise multiplication of two vectors and $\boldsymbol{\iota}$ accounts for the effects of biaxial interaction. The vectors $\boldsymbol{\beta}$ and $\boldsymbol{\gamma}$ are parameters which govern the hysteretic behavior of the system and are given as $\boldsymbol{\beta} = [\boldsymbol{\beta_1}, \ldots, \boldsymbol{\beta_n}]^{\boldsymbol{T}}$ and$\boldsymbol{\gamma} = [\boldsymbol{\gamma_1}, \ldots, \boldsymbol{\gamma_n}]^{\boldsymbol{T}}$. The parameter $\boldsymbol{\eta}$ which is defined as the sharpness of the hysteretic knee which governs the smoothness of the transition from the linear to the nonlinear range [11]; this helps in adjusting the knee of the hysteresis loop. The yield displacement is given by

$$\boldsymbol{z_{i,yield}} = \frac{\boldsymbol{1}}{\sqrt[\boldsymbol{n}]{\boldsymbol{\beta_i} + \boldsymbol{\gamma_i}}} \tag{26}$$

The hysteretic shape parameter, $\rho \in [0, 1]$, and

$$\boldsymbol{\beta_i} = \frac{\boldsymbol{\rho}}{\boldsymbol{z_{i,yield}^{\eta}}} \text{ and } \boldsymbol{\gamma_i} = \frac{\mathbf{1} - \boldsymbol{\rho}}{\boldsymbol{z_{i,yield}^{\eta}}} \tag{27}$$

Substituting the above equations into the relative equations of motion we get

$$\widetilde{\boldsymbol{M_u}}\ddot{\boldsymbol{u}} + \widetilde{\boldsymbol{C}}_{\boldsymbol{u}}\dot{\boldsymbol{u}} + \widetilde{\boldsymbol{\kappa K_u}}\boldsymbol{u} + (\mathbf{1} - \boldsymbol{\kappa})\widetilde{\boldsymbol{K_u}}\boldsymbol{z} = -\tilde{\boldsymbol{\mu}}\ddot{\boldsymbol{u}}_{\boldsymbol{g}} \tag{28}$$

Premultiplying the above Equation by $\boldsymbol{T^{-T}}$ and substituting the expression for $\boldsymbol{u_x}$ from Equation (18), we transform the equations of motion back to absolute coordinates

$$\widetilde{\boldsymbol{M}}\ddot{\boldsymbol{x}} + \widetilde{\boldsymbol{C}}\dot{\boldsymbol{x}} + \boldsymbol{\kappa}\widetilde{\boldsymbol{K}}\boldsymbol{x} + (\mathbf{1} - \boldsymbol{\kappa})\widetilde{\boldsymbol{K}}\boldsymbol{z} = -\tilde{\boldsymbol{\mu}}\ddot{\boldsymbol{u}}_{\boldsymbol{g}} \tag{29}$$

Where

$$\dot{\boldsymbol{z}}_{\boldsymbol{x}} = \boldsymbol{T^{-1}}\dot{\boldsymbol{x}} - \boldsymbol{z} \text{ o } \boldsymbol{\iota} \tag{30}$$

$$\boldsymbol{\iota} = \{\boldsymbol{\beta}\ \boldsymbol{o}\ \boldsymbol{abs}\ [(\boldsymbol{T^{-1}}\dot{\boldsymbol{x}})\boldsymbol{o}\ \boldsymbol{z}] - \boldsymbol{\gamma}\ \boldsymbol{o}\ (\boldsymbol{T^{-1}}\dot{\boldsymbol{x}})\boldsymbol{o}\ \boldsymbol{z}\}\boldsymbol{o}\ (\boldsymbol{z}\ \boldsymbol{o}\ \boldsymbol{z})^{\frac{\boldsymbol{\eta}-\mathbf{2}}{\mathbf{2}}} \tag{31}$$

The values of these hysteretic parameters are obtained by fitting pulse responses of the condensed model to pulse responses of the detailed model. Specifically, a short-period pulse (with a period of about half the fundamental period of the structure) is applied to the high-fidelity model to generate inter-story drift ratio time histories. The pulse amplitude is large enough to produce inter-story drift ratios up to three or four percent in the lower stories. The same pulse is applied to the condensed model and inter-story drift ratios are computed from the reduced order model. The condensed

model is then fit to the high fidelity model via nonlinear least squares. The Levenberg-Marquardt method is used to solve the nonlinear least squares problem.

4.3 Step 3: Hysteretic Parameters Approximation

In order identify estimates of the hysteretic parameters for the condensed model that would result in good predictions of the high-fidelity model, hysteretic parameters were fit to high-fidelity response data computed for a number of different loading types, including quasi-static push over loading and dynamic impulsive loading. The best set of parameters was obtained from fitting responses that involved higher modes. This was finally achieved using a high amplitude pulse response data. To be certain of which type of analysis would be appropriate a trial and error method was utilized.

The first method of obtaining the hysteretic parameters involved a pushover analysis of the detailed and the condensed model. Using a uniform Static loading (the same lateral force at each floor level), the load-displacement curves obtained from the condensed model were fitted to respect to the high-fidelity model responses using the Levenberg-Marquardt method. The condensed model with the fitted parameter values was then tested by comparing hysteretic earthquake ground motion responses predicted by the fitted condensed model to those computed with the high-fidelity model., The error in the peak horizontal displacements between the high-fidelity model and the fitted condensed model when subjected to an earthquake ground motion loading was

as large as 40%. This was due to the fact that higher modes and cyclic hysteretic behavior were not involved in the pushover analysis responses.

The next method involved a quasi-static pushover analysis, which involved a slow acceleration in the base response. The fitted hysteretic parameters obtained were then tested; the elastic response of the High Fidelity OpenSees model seemed to match the condensed Matlab model. But the inelastic response still had an error which needed to be addressed.

Finally, the detailed and the condensed model were subjected to a high amplitude pulse response. The high amplitude pulse had a ground motion pulse period of 0.5 sec, half of the fundamental period of the structure. The inter-story drift plots for the High Fidelity OpenSees model and the Condensed Hysteretic model were computed.

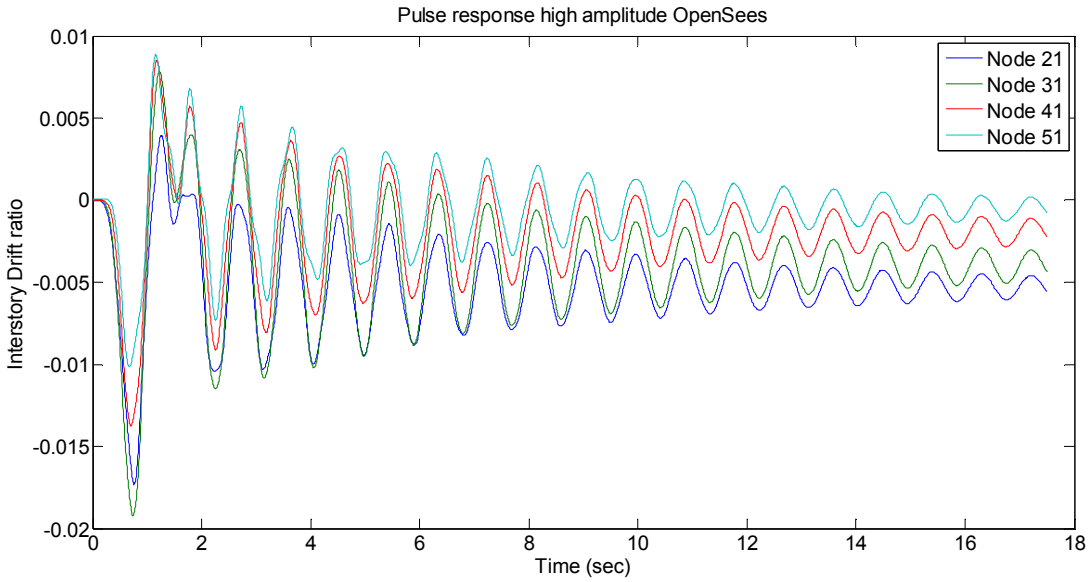

Figure 4: Inter-story Drift ratio for the High Amplitude Pulse Response of the High Fidelity OpenSees model.

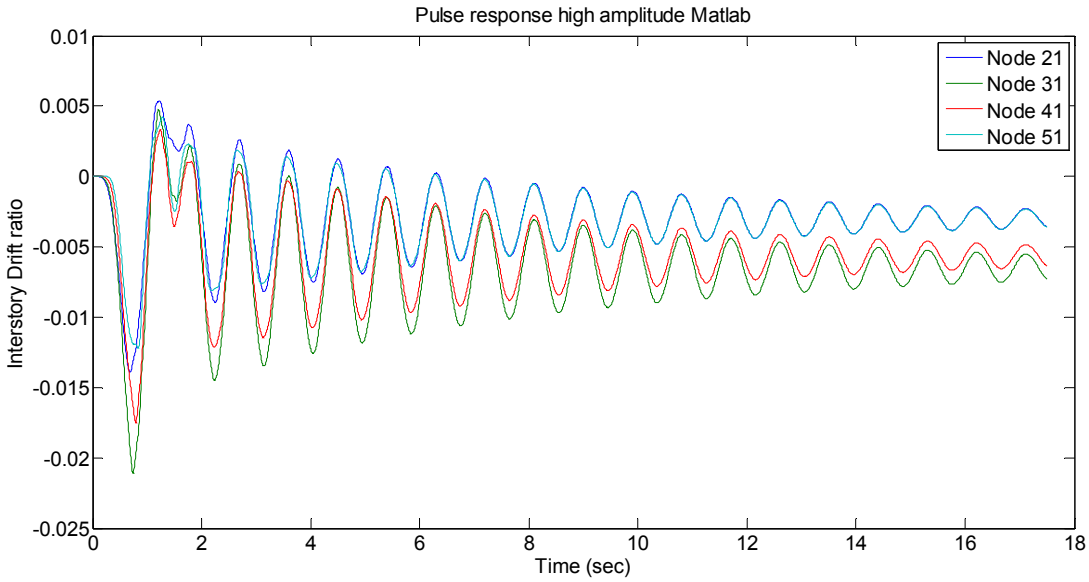

Figure 5: Inter-story Drift ratio for the High Amplitude Pulse Response of the Condensed Hysteretic model using initial guess for the hysteretic parameters.

4.4 Step 4: Fit the Reduced inelastic model response data from the high fidelity model using the Levenberg-Marquardt algorithm.

The Levenberg-Marquardt is a technique used to solve nonlinear least square problems [13]. Least squares problems arise when fitting a parameterized function to a set of measured data points by minimizing the sum of the squares of the errors between the data points and the function. In such a case, the function is not linear in the parameters. The Parameters values are modified in an iterative procedure to reduce the sum of the squares of the errors between the measured data points and the function. The Levenberg-Marquardt method involves a combination of the gradient descent method and the Gauss-Newton method.

The gradient descent method updates the parameters in the direction of the greatest reduction of the least squares objective by reducing the sum of the squared errors. Whereas, In the Gauss-Newton method, the sum of the squared errors is reduced by assuming the least squares function is locally quadratic whose minimum is to be obtained. Using this combination of methods, the Levenberg-Marquardt method uses a mixture of these methods depending upon the difference between the parameters from their optimal value. If the difference between the parameters and the optimal value is large then the gradient descent method is used and as the difference between the parameters and the optimal value reduces, the Gauss-Newton method is used. This

combination is an efficient way to minimize the sum of the squares of the errors between the data points and the function.

In fitting a function $\hat{y}\ (t; \boldsymbol{p})$ of an independent variable $\boldsymbol{t}$ and a vector of $\boldsymbol{n}$ parameters $\boldsymbol{p}$ to a set of m data points (t_i, y_i), the minimization sum of the weighted squares of the errors between the measured data $y(t_i)$ and the curve-fit function $\hat{y}\ (t_i; \boldsymbol{p})$ is performed. This scalar-valued goodness-of-fit measure is called the chi-squared error criterion.

$$\chi^2 = \sum_{i=1}^{n} \left[\frac{y(t_i) - \hat{y}(t_i; p)}{\omega_i} \right]^2 \tag{1}$$

$$= (y - \hat{y}(p))^T W (y - \hat{y}(p)) \tag{2}$$

$$= y^T W y - 2y^T W \hat{y} + \hat{y}^T W y' \tag{32}$$

The error in data point $y(t_i)$ is weighted by the value ofω_i. The weighting matrix W is diagonal with $W_{ii} = 1/{\omega_i}^2$. The minimization of χ^2 with respect to the parameters is carried out iteratively. The goal of each iteration is to find a perturbation $\boldsymbol{h}$ to the parameters $\boldsymbol{p}$ that reducesχ^2.

The Gradient Descent Method

The gradient descent method updates the parameter values in the direction opposite to the gradient of the objective function. It is recognized as a highly convergent algorithm for finding the minimum of simple objective functions [17] [18]

The gradient of the chi-squared objective function with respect to the parameters is

$$\frac{\partial}{\partial \boldsymbol{p}} \chi^2 = (y - \hat{y}(\boldsymbol{p}))^T W \frac{\partial}{\partial \boldsymbol{p}} (y - \hat{y}(\boldsymbol{p})) \tag{4}$$

$$= -(\boldsymbol{y} - \hat{\boldsymbol{y}})^{\boldsymbol{T}} \boldsymbol{W} \boldsymbol{J} \tag{5}$$

Where the *m x n* Jacobian matrix $[\delta\hat{y} / \delta\boldsymbol{p}]$represents the local sensitivity of the function $\hat{y}$ to variation in the parameters$\boldsymbol{p}$, and *J* represents $[\delta\hat{y} / \delta\boldsymbol{p}]$. The perturbation $\boldsymbol{h}$ that moves the parameters in the direction of the steepest descent is given by

$$h_{gd} = \alpha J^T W (y - \hat{y}) \tag{6}$$

Where, α determines the length of the step in the steepest-descent direction.

The Gauss-Newton Method

The Gauss-Newton method is used for minimizing the sum of squares objective function. It assumes the objective function is approximately quadratic in the parameters near the solution [18]. The Gauss-Newton method converges faster than the Gradient Descent method [19]. The perturbation $\boldsymbol{h}$ that minimizes χ^2 is found from $[\delta\chi^2 / \delta\boldsymbol{h}] = 0$.

$$\frac{\partial}{\partial h} \chi^2 (p + h) \cong -2 (y - \hat{y})^T W J + 2h^T J^T W J \tag{7}$$

And the resulting normal equations for the Gauss-Newton perturbation are

$$[J^T W J] h_{gn} = J^T W (y - \hat{y}) \tag{8}$$

The Levenberg-Marquardt Method

The Levenberg-Marquardt algorithm varies the parameter changes between the gradient descent update and the Gauss-Newton update. Marquardt's suggested update relationship is as follows [20]

$$[J^T W J + \lambda\, diag(J^T W J)]h_{lm} = J^T W (y - \hat{y}) \quad (9)$$

This algorithm was used in finding the values of the hysteretic parameters used in the model reduction technique for nonlinear inelastic analysis.

The curve fitting was initially done using a quasi-static pushover analysis of the high-fidelty OpenSees model with the condensed hysteretic model. Since the hysteretic parameters obtained from fitting the quasi-static pushover response data did not lead to a condensed model that could predict the high-fidelity model responses to earthquake ground motion , the curve fitting was then carried out using high amplitude pulse response data.

Quasi-static Analysis

Quasi-static loading is a type of a linear time-varying loading that increases slowly with time. The high-fidelity (OpenSees) frame model and the condensed model were subjected quasi-static loading. The responses of both models exhibited clear plastic deformation. The inter-story drift ratios versus time were plotted in both cases. Curves that were obtained from the condensed model were fitted to data from the full model in order to estimate values of the hysteretic parameters. The figures below show the plots between the inter-story drift ratio and time for the high-fidelity model and the condensed model.

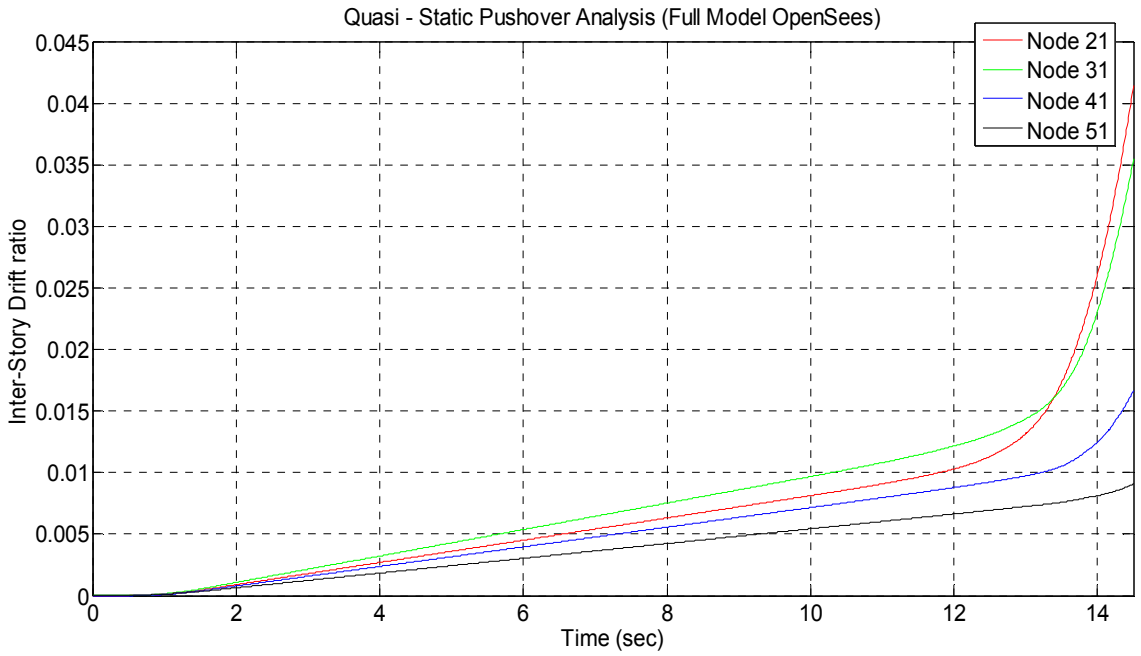

Figure 6: Inter-story Drift ratio plot for the Quasi-Static Pushover Analysis of the High Fidelity OpenSees model.

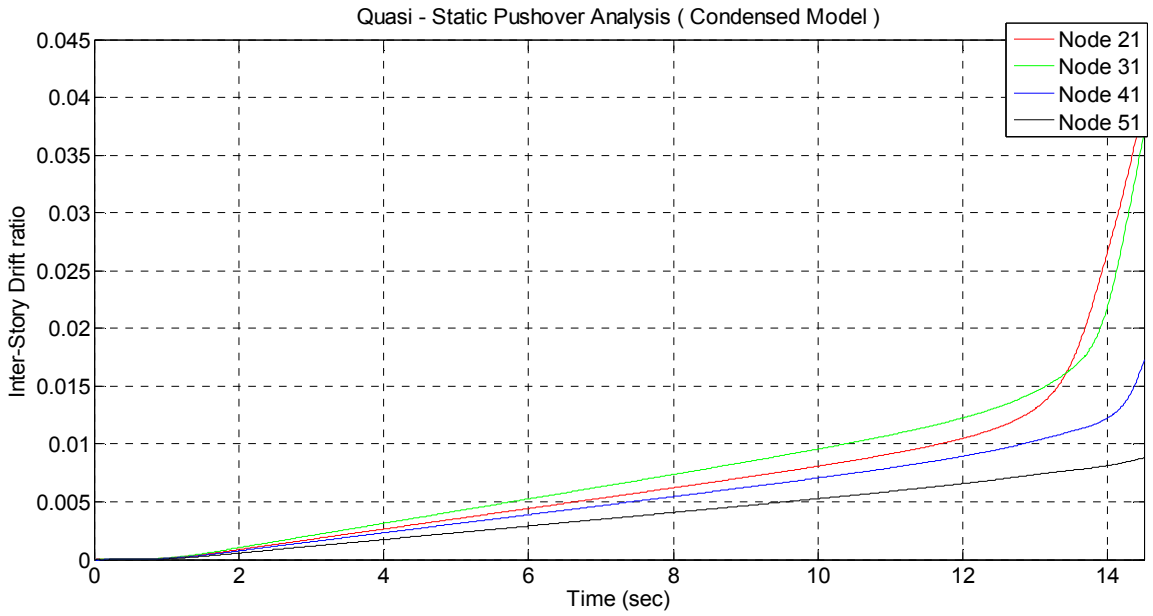

Figure 7: Inter-story Drift ratio plot for the Quasi-Static Pushover Analysis of the Condensed model.

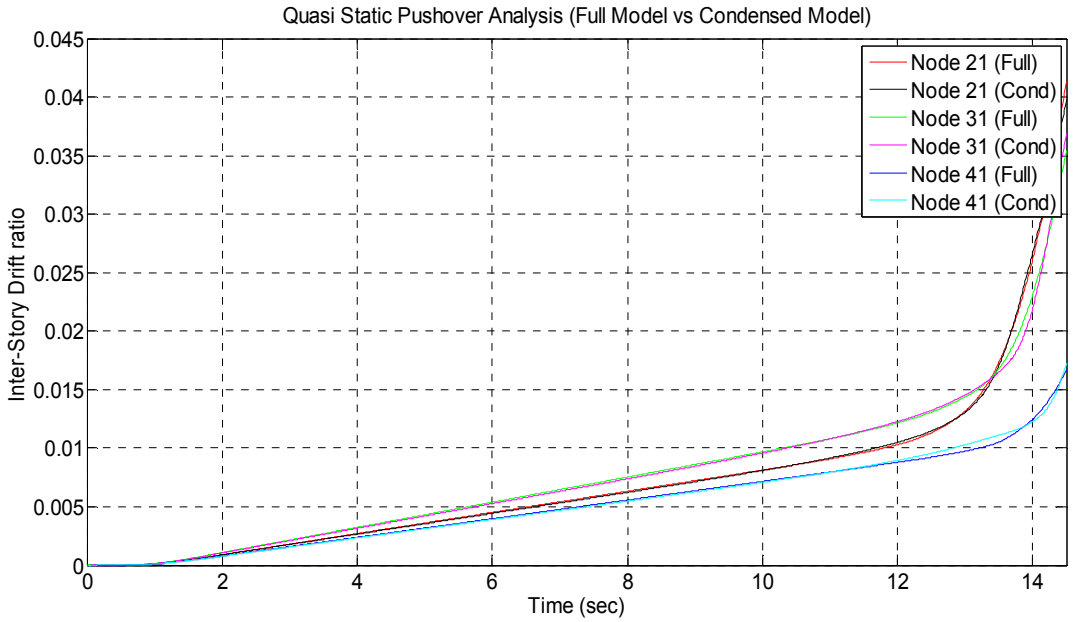

Figure 8: Inter-Story Drift ratio plot showing the difference between the two models.

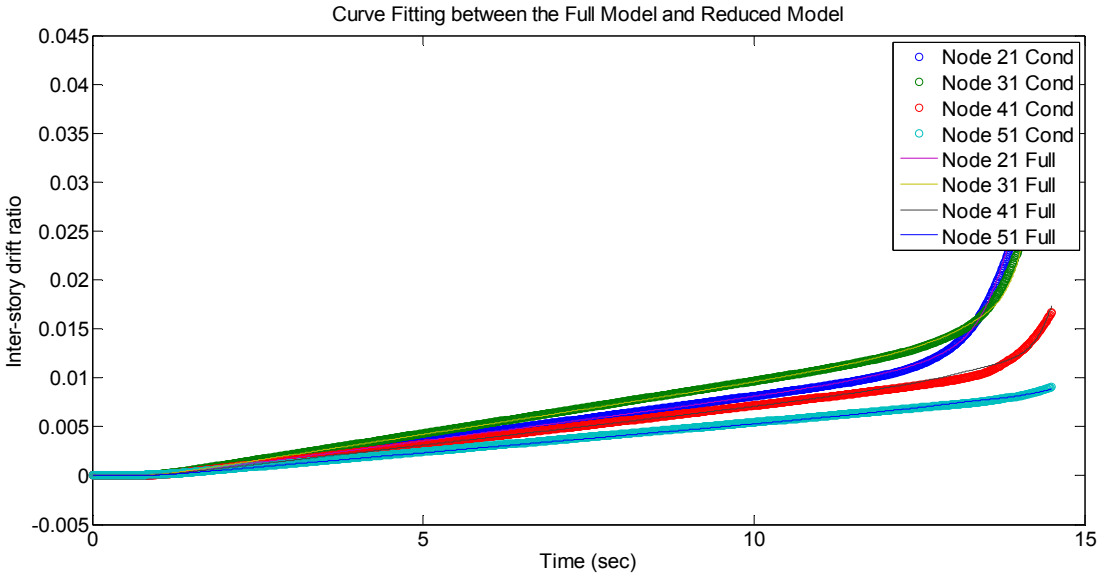

Figure 9: Curve-Fitting of the High Fidelity model response with the Condensed model response in order to obtain fitted hysteretic parameters.

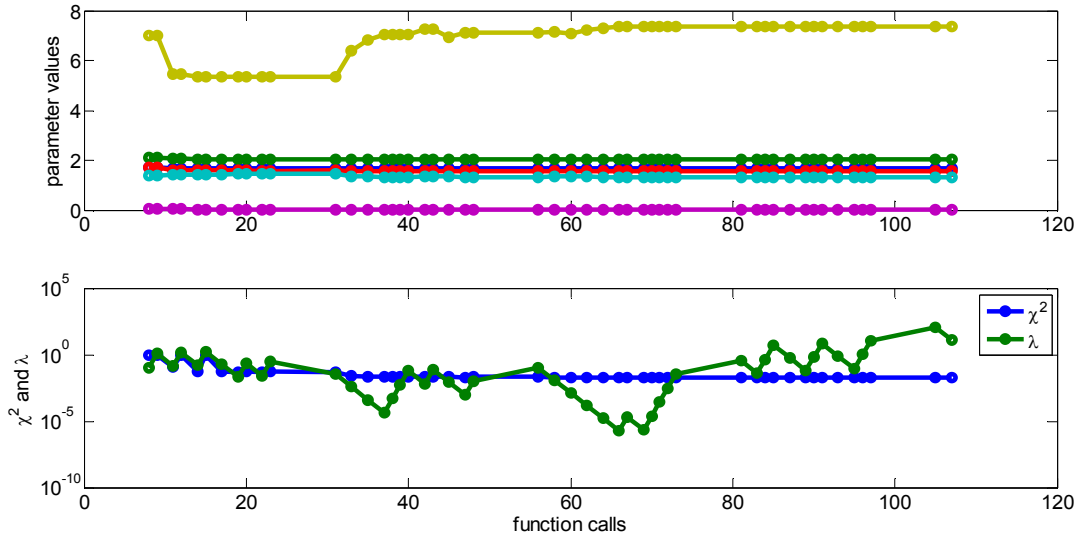

Figure 10: Variation in the Hysteretic Parameters during the curve fitting process.

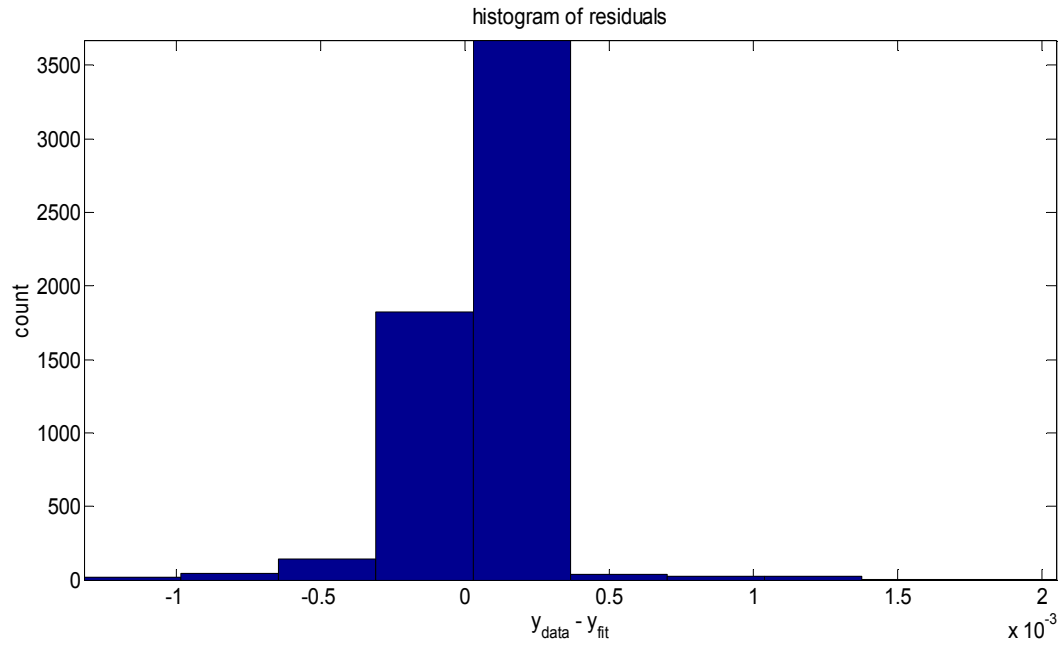

Figure 11: Histogram of the residuals after the completion of the curve fitting.

The verification of these hysteretic parameters is given in the next chapter. The condensed model with hysteretic parameters obtained by the fitting of the quasi-static pushover curves was successful in predicting an identical dynamic elastic response as the high-fidelity model but failed to show the same accuracy when subjected to loadings that produced inelastic behavior.

The reason of the failure of the hysteretic parameters obtained by curve fitting the quasi-static pushover curve can be due to the following aspects missing in the pushover analysis:

- Dynamic Behaviour
- Multi-Mode Behaviour
- Cyclic Hysteretic Behaviour
- Residual Displacement

Thus, a high amplitude pulse response analysis was carried out on the two models. The inter-story drift ratio curve of the condensed hysteretic model using some initial parameters was fitting with the curve obtained from the high-fidelity OpenSees model.

The fitted hysteretic parameters are as follows:

κ= 0.02

z_{yield}= [1.6780, 2.1897, 1.8404, 1.7491] in.

η= 12.000

ρ= 0.5

These hysteretic parameters were used for the condensed hysteretic model and an inelastic response was obtained. The condensed hysteretic model was verified for a

set of earthquake records and its accuracy with respect to the detailed model was checked, as described in the next chapter.

5. Model Verification:

Several stages of model verification were carried out. First the high-fidelity model was verified in terms of its low-amplitude dynamic elastic behavior, by comparing its modal frequencies and low-amplitude earthquake dynamic response histories to those computed from a linear 2D elastic frame analysis. Second, the high-fidelity model was verified in terms of its high-amplitude static inelastic behavior by comparing its pushover analysis to those computed from an independent pushover analysis in which inelastic behavior is concentrated at plastic hinges at the nodes and elastic-plastic moment-curvature relationships are assumed at these nodes.

5.1 Verification of elastic dynamic response: 2D Elastic Frame Model and the High Fidelity OpenSees Model

First, the low-amplitude dynamic elastic behavior of the high-fidelity model generated in OpenSees was verified in comparison to an elastic 2D frame model.

Table 1: Natural Frequencies of the High Fidelity OpenSees model, Elastic Frame model and Condensed Hysteretic model

Natural Frequency	High Fidelity OpenSees model (Hz)	Elastic Frame Model (Hz)	Condensed Hysteretic Model (Hz)
f_{n1}	1.1035	1.1093	1.1093
f_{n2}	3.1208	3.1430	3.2769
f_{n3}	5.7544	5.7959	6.5261
f_{n4}	8.5398	8.6181	10.4412

Natural Periods of the High Fidelity OpenSees model, Elastic Frame model and Condensed Hysteretic Matlab model:

Table 2: Natural Periods of the High Fidelity OpenSees model, Elastic Frame model and Condensed Hysteretic model

Natural Period	High Fidelity OpenSees model (sec)	Elastic Frame Model (sec)	Condensed Hysteretic Model (sec)
T_{n1}	0.9062	0.9014	0.9014
T_{n2}	0.3204	0.3182	0.3051
T_{n3}	0.1738	0.1725	0.1532
T_{n4}	0.1171	0.1161	0.0958

Next a comparison was made in terms of low-amplitude dynamic responses. The ground motion record for this analysis was obtained from the PEER Ground Motion Database [24].

Table 3: Peak Ground Acceleration of the different NGA ground motion used:

Ground Motion	Scaled Peak Ground Acceleration (PGA) (g)
NGA 0181	1.108
NGA 0182	0.648
NGA 0292	0.862
NGA 0723	0.709
NGA 0802	1.253
NGA 0821	0.593
NGA 0879	1.679
NGA 1063	0.569
NGA 1086	0.604
NGA 1165	0.486
NGA 1503	1.058
NGA 1529	0.595
NGA 1605	0.871

One of the ATC-63 near Fault Ground Motion Records [25] with a pulse was used on both the models; record NGA0181 was selected with a scaling factor of 0.9. Figure 10 shows the ground motion acceleration against time. Figure 11 shows the seismic response of the high-fidelity OpenSees model in the form of a horizontal displacement time histories. The horizontal displacements for nodes 21, 31, 41 and 51 are shown for further comparison with the elastic 2D frame model. Figure 14 shows the seismic response of the elastic 2D frame model in the form of a lateral horizontal displacement versus time plot as well.

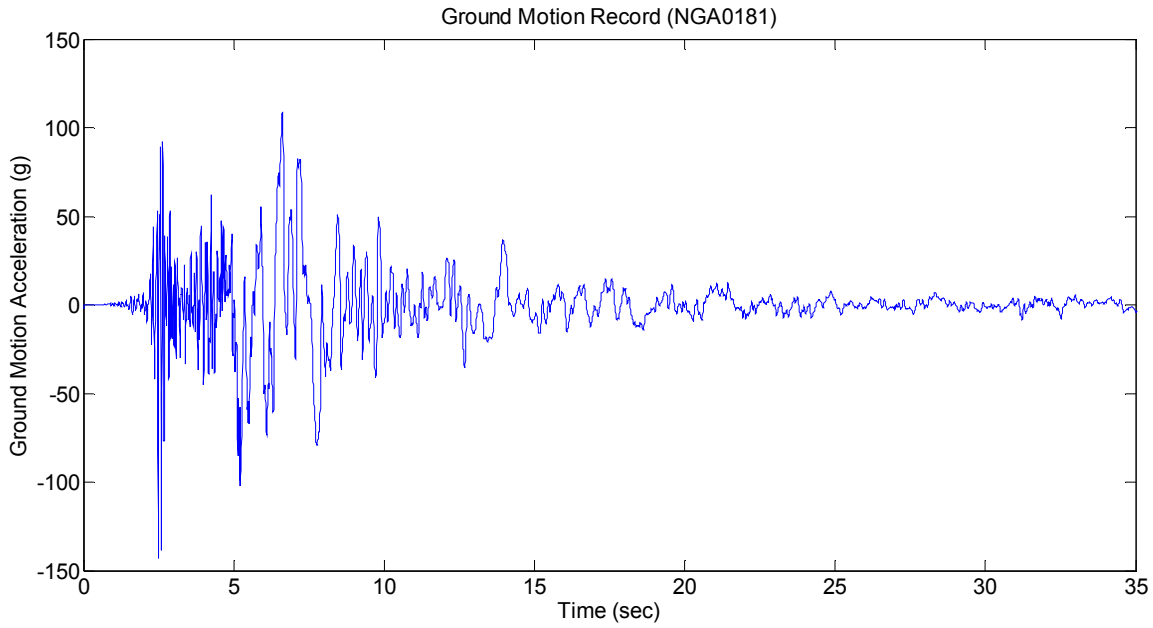

Figure 12: Ground Motion Record used for the dynamic analysis.

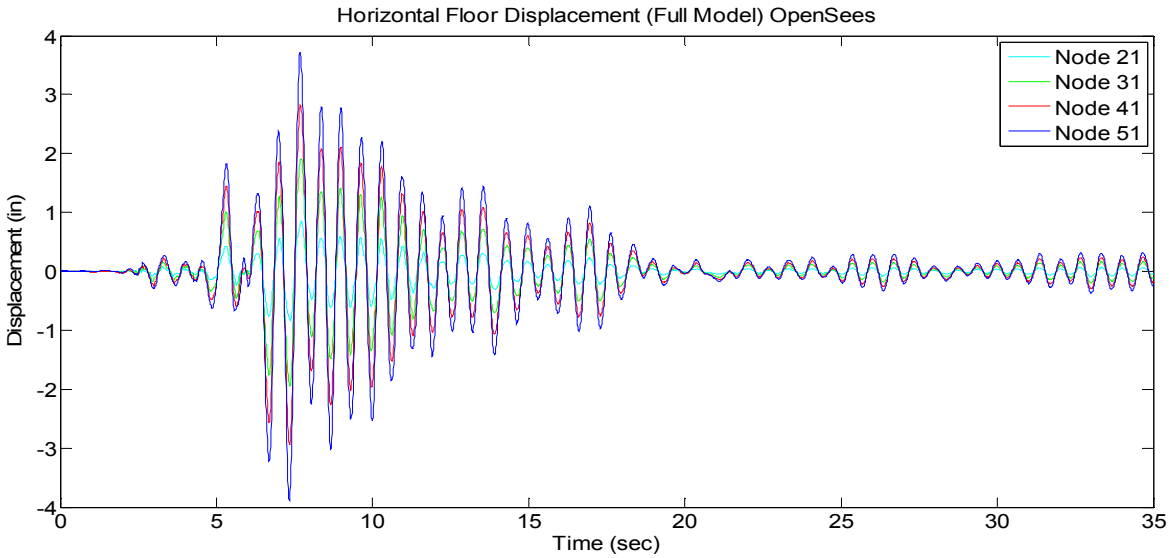

Figure 13: Horizontal Floor Displacement for the OpenSees model – elastic response

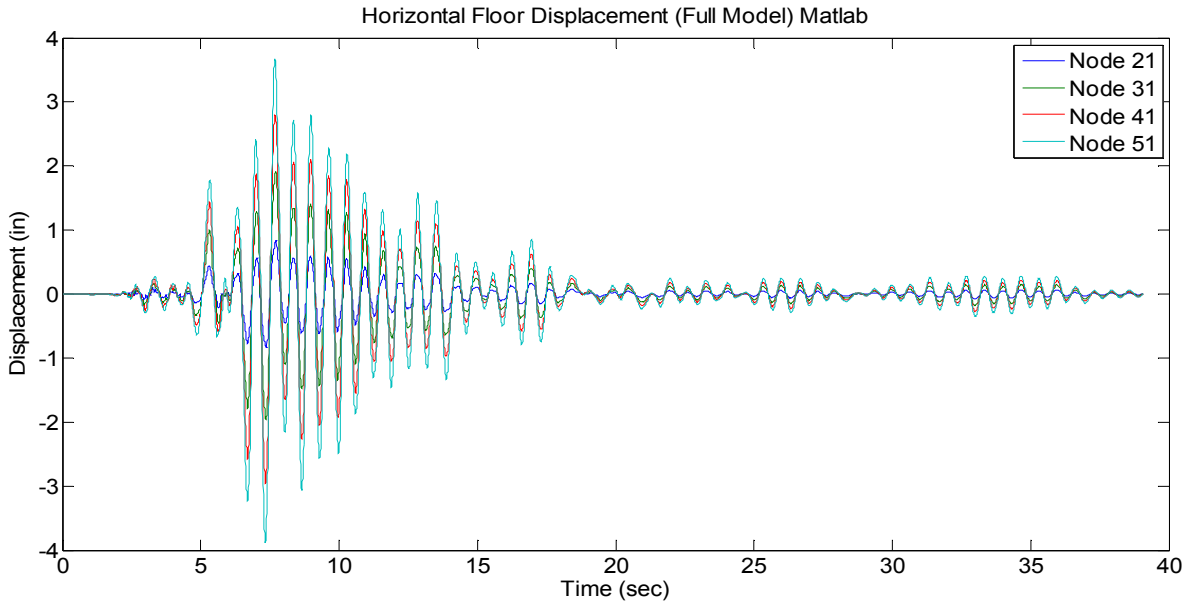

Figure 14: Horizontal Floor Displacement for the Elastic Frame model – elastic response

The peak response for the Opensees Model occurs at node 51 and is equal to -3.8825. The peak response for the 2D elastic frame model occurs at node 51 and is equal to -3.8829. Thus, on the basis of these two factors, the elastic dynamic response of the OpenSees and the Matlab model is very similar. The next step in verifying these two models will be by using the Guyan Dynamic Reduction (Paz Reduction) that has been discussed in the earlier chapters.

5.2 Linear elastic model reduction: comparing the OpenSees Full model with the 2D elastic frame and elastic reduced-order model models.

The 2D elastic frame model is then reduced from sixty coordinates to four horizontal coordinates using the Dynamic Condensation method. As discussed earlier, the mass and the stiffness matrices are condensed using the transformation matrix. This reduction of the number of degrees of freedom results in an accurate and efficient seismic response for a linear elastic dynamic analysis. Figure 15 shows the seismic response of the condensed elastic model in the form of lateral horizontal displacement time histories for the four coordinates that are retained.

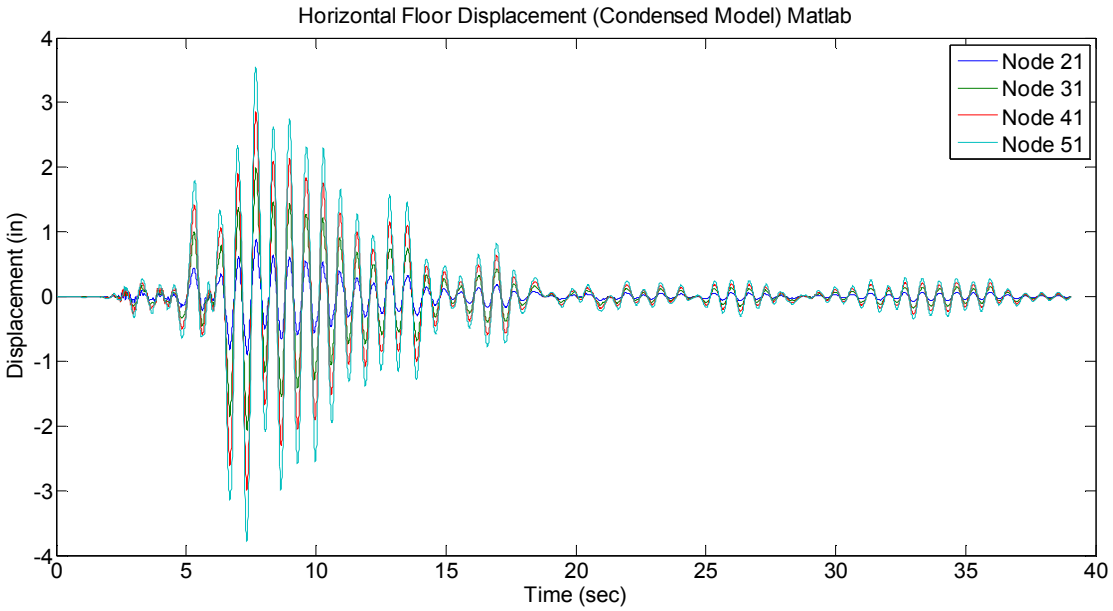

Figure 15: Horizontal Floor Displacement for the Matlab Condensed Elastic model – elastic response

The peak response for the condensed elastic model is the same as the peak response for the high fidelity model. The natural frequencies in the lower modes also match, but on evaluating the higher modes, the difference in natural frequency of the high fidelity model and the condensed elastic model seem to increase. Since the linear elastic dynamic analysis is within the elastic region, the higher mode shapes can be ignored for now.

5.3Verification of the inelastic pushover response of the full model – EPFrame and OpenSees pushover analysis:

The inelastic behavior of the high fidelity model was verified using static pushover analysis. The structure is subjected to lateral forces which are distributed over height. The distribution can be done in several ways according to the FEMA-273 [1] load distribution. FEMA-273 specifies three distributions for lateral forces:

- Mass-proportional lateral load distribution : $s_n^* = m_n$, the mass at the n^{th} floor level (where the floor number n = 1,2, …, *N*)
- Equivalent Lateral Force for Distribution (ELF): $s_n^* = m_n h_n^k$ where h_n is the height of the n^{th} floor level above the base, and the exponent k = 1 for fundamental period $T_1 \leq 0.5$ sec, k = 2 for $T_1 \geq 2.5$ sec; and varies linearly between the presented range
- SRSS distribution: s^* is defined by the lateral forces calculated from the story shears determined by the response spectrum analysis of the structure, which is assumed to be linearly elastic.

A uniform distribution of loads of assumed in this verification process. The static pushover analysis of the model computed by the high-fidelity OpenSees model was verified by performing the same analysis on a FORTRAN program named EPFrame [26]. The structure was subjected to equal horizontal loads at nodes 21, 31, 41 and 51. The load deflection plots that were generated were compared to determine the inelastic behavior of the structure under static loading.

EPFrame returns the load-deflection relationships of elastic-plastic analysis Figure 16 to 19 show the load-deflection plots of nodes 21, 31, 41 and 51 for both the OpenSees values as well as the EPFrame values. It can be concluded from these plots

that the elastic-plastic behavior for the frame under static loading is the same in both the cases, and the high-fidelity model is thus verified for static pushover loading, well into the inelastic range.

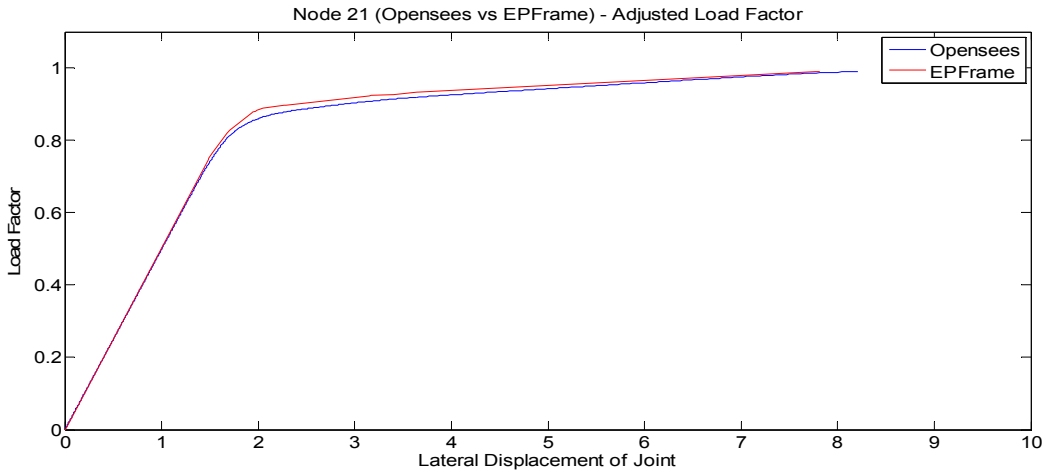

Figure 16: Load – Deflection plot for node 21 showing the comparison between the inelastic pushover response in OpenSees and EPFrame.

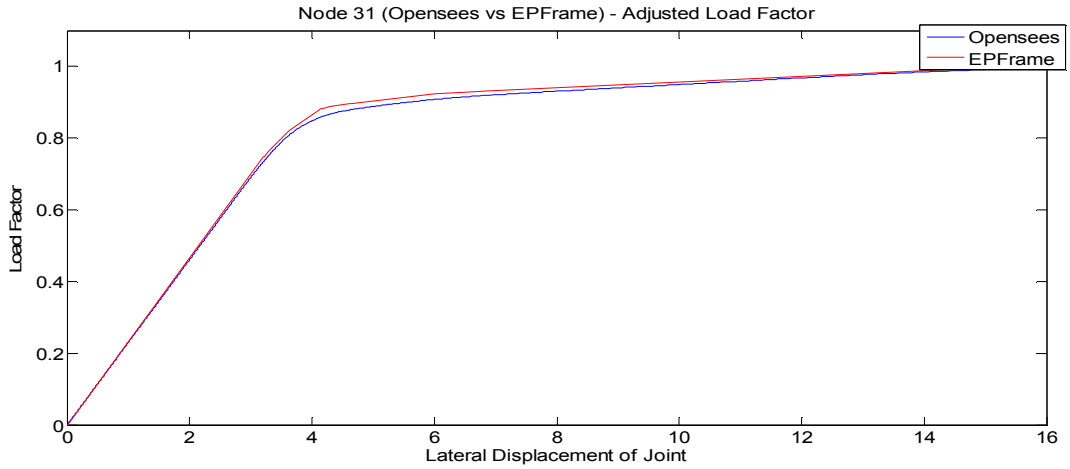

Figure 17 : Load – Deflection plot for node 31 showing the comparison between the inelastic pushover response in OpenSees and EPFrame.

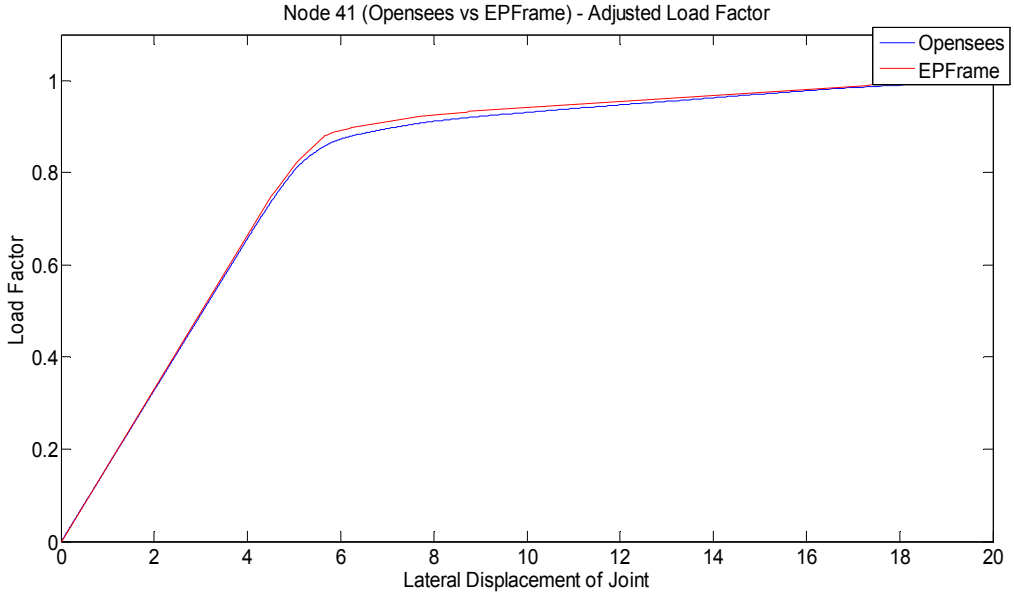

Figure 18: Load – Deflection plot for node 41 showing the comparison between the inelastic pushover response in OpenSees and EPFrame

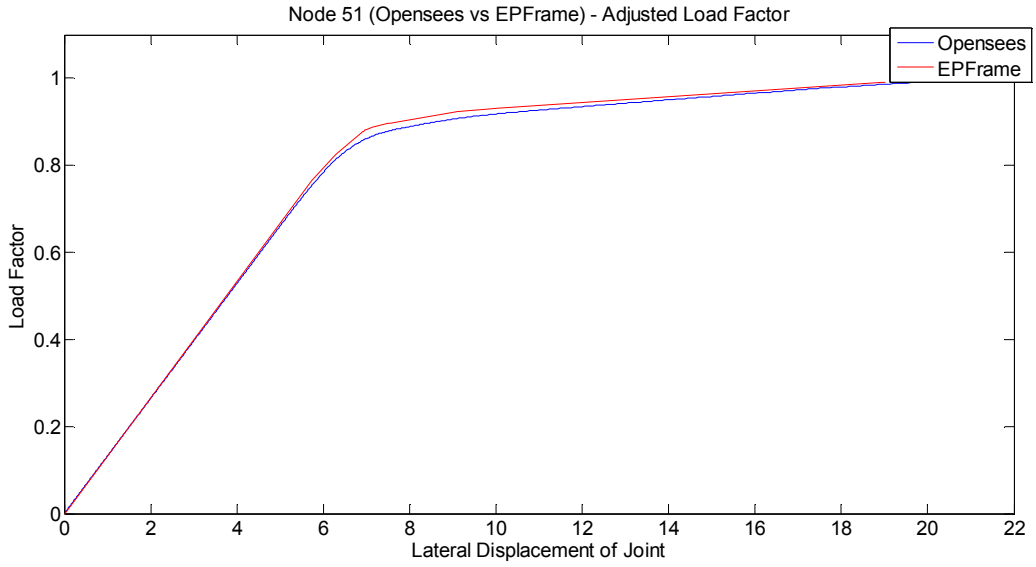

Figure 19: Load – Deflection plot for node 51 showing the comparison between the inelastic pushover response in OpenSees and EPFrame

5.4 Verification of the Condensed Hysteretic Model

The inelastic dynamic response was first verified for the hysteretic parameters obtained from the quasi-static pushover analysis. Since the error in the inelastic region was large, the new hysteretic parameters were obtained using the high amplitude pulse response. In this section, the dynamic elastic analysis of the different hysteretic parameters obtained will be discussed

Using the Levenberg-Marquardt method the hysteretic parameters from the static pushover curve fitting are given in the table below:

Table 4: Hysteretic Parameters obtained from the static pushover curve fitting

	Initial	Fit	σ_p	% Change
$z_{yield,1}$	1.7	1.6754	0.0003	0.0161
$z_{yield,2}$	2.1	2.0347	0.0002	0.0085
$z_{yield,3}$	1.7	1.5555	0.0004	0.0250
$z_{yield,4}$	1.4	1.3325	0.0023	0.1758
κ	0.05	0.0335	0.0001	0.4172
η	7	7.3660	0.0278	0.3770

These fitted hysteretic parameters are used and all three models are subjected to dynamic analysis. The figure 20 show the lateral displacement versus time plots for the selected nodes of the High Fidelity Model, The Elastic Frame Model and the Condensed

Hysteretic Model. Moment Rotation curves have also been plotted to further understand the hysteretic behavior of the structure under high intensity ground acceleration.

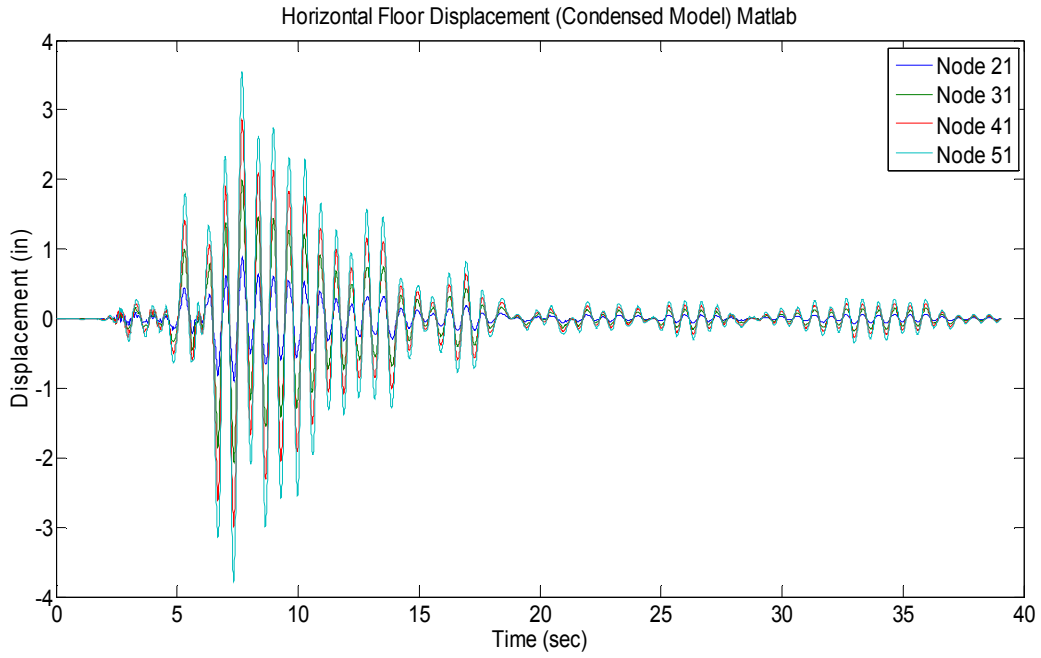

Figure 20: Elastic Earthquake Response of the Hysteretic Condensed model obtained using Quasi-Static Pushover response

Table 5: Hysteretic Parameters obtained by the Quasi-Static Pushover curve fitting:

	Initial	Fit	σ_p	% Change
$z_{yield,1}$	1.6320	1.6780	0.0003	2.818
$z_{yield,2}$	1.9994	2.1897	0.0002	9.51
$z_{yield,3}$	1.5778	1.8404	0.0004	16.64
$z_{yield,4}$	1.3586	1.7491	0.0023	28.74
κ	0.0688	0.0200	0.0001	70.93
η	7.2843	12.000	0.0278	64.73

These Fitted Hysteretic Parameters are used instead of the initial assumptions and all the three models are subjected to dynamic analysis. The Figure 21 below show the Lateral Displacement versus time plots for the selected nodes of the OpenSees Model, The Elastic Frame Model and the Condensed Hysteretic Matlab model. Moment Rotation curves have also been plotted to further understand the hysteretic behavior of the structure under high intensity ground acceleration.

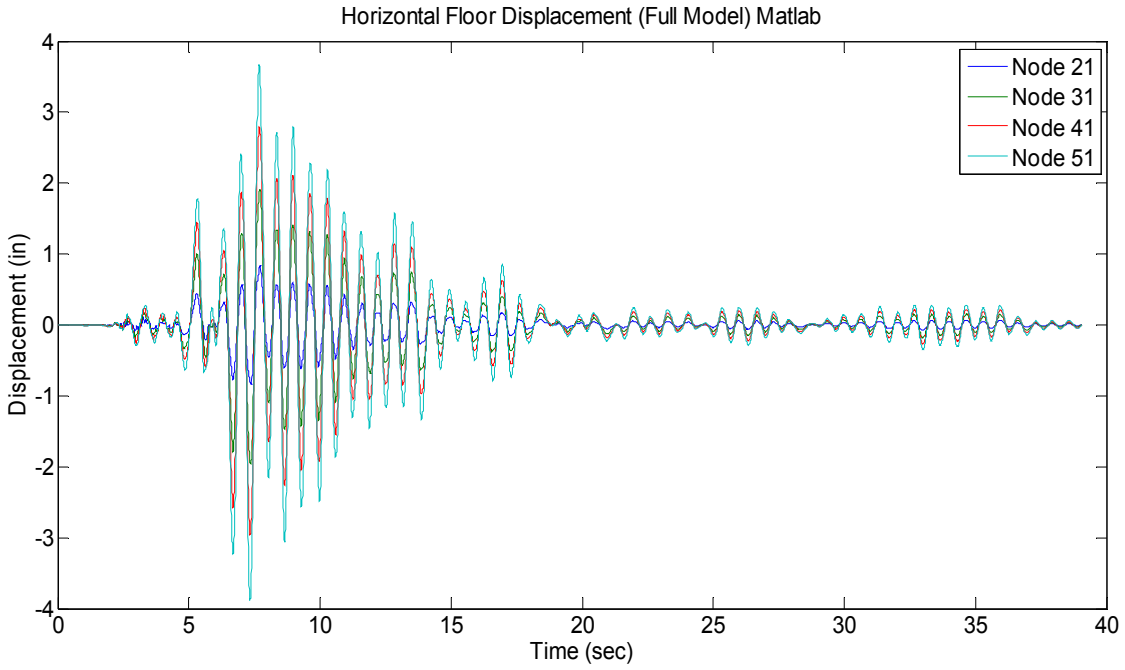

Figure 21: Horizontal Floor Displacement from the 2D elastic frame model

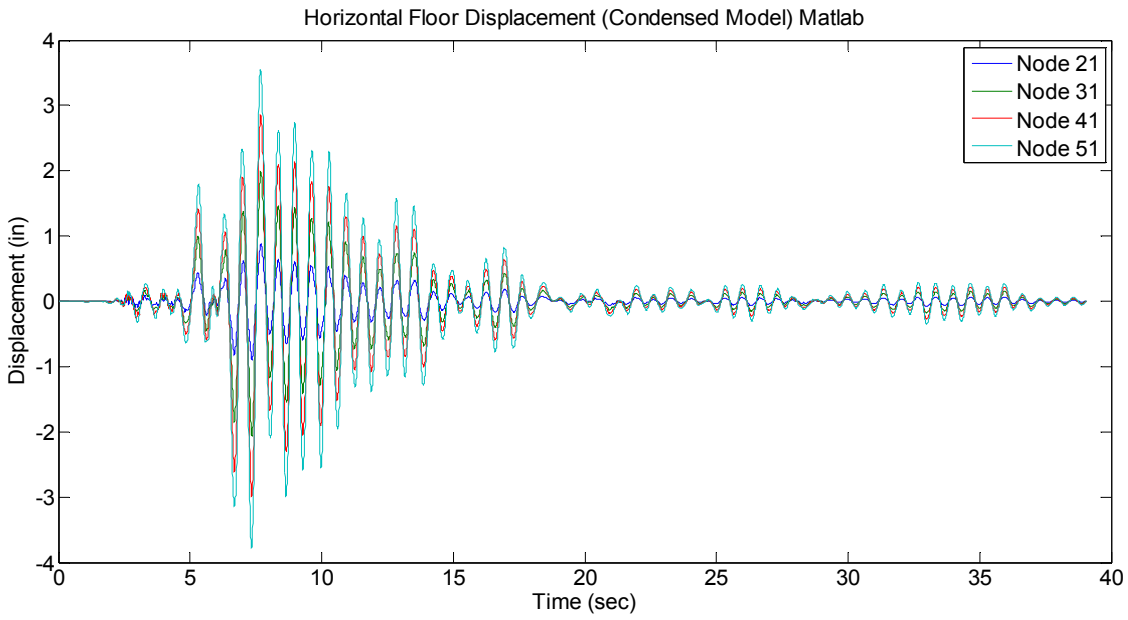

Figure 22: Horizontal Floor Displacement from the Condensed Hysteretic model with parameters fit to the High Amplitude Pulse Response

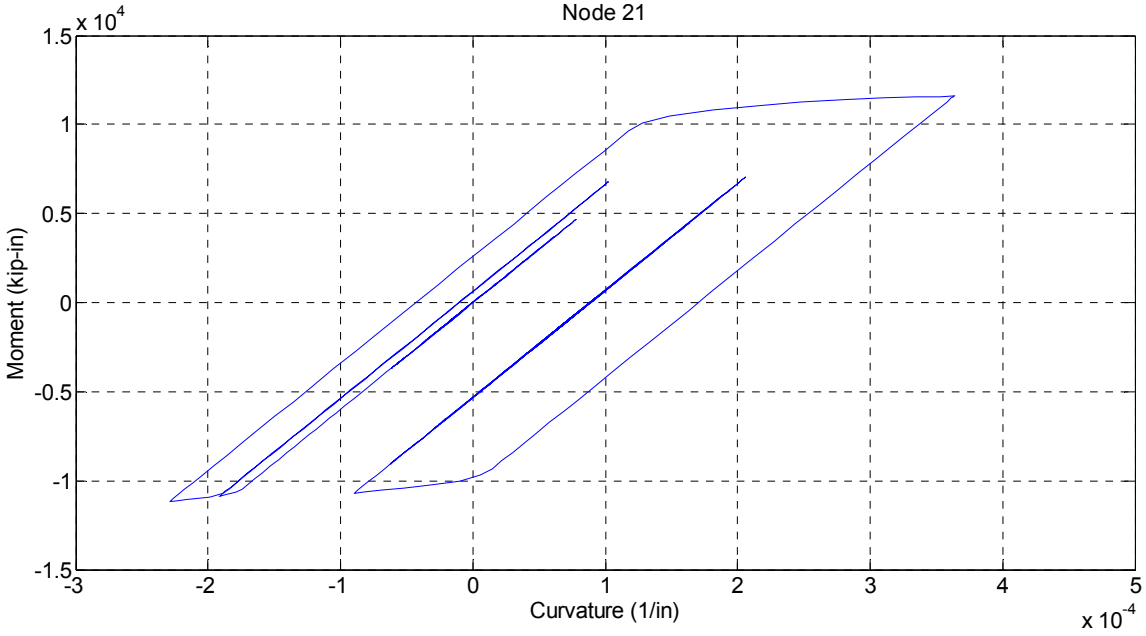

Figure 23: Moment Curvature Hysteresis Node 21

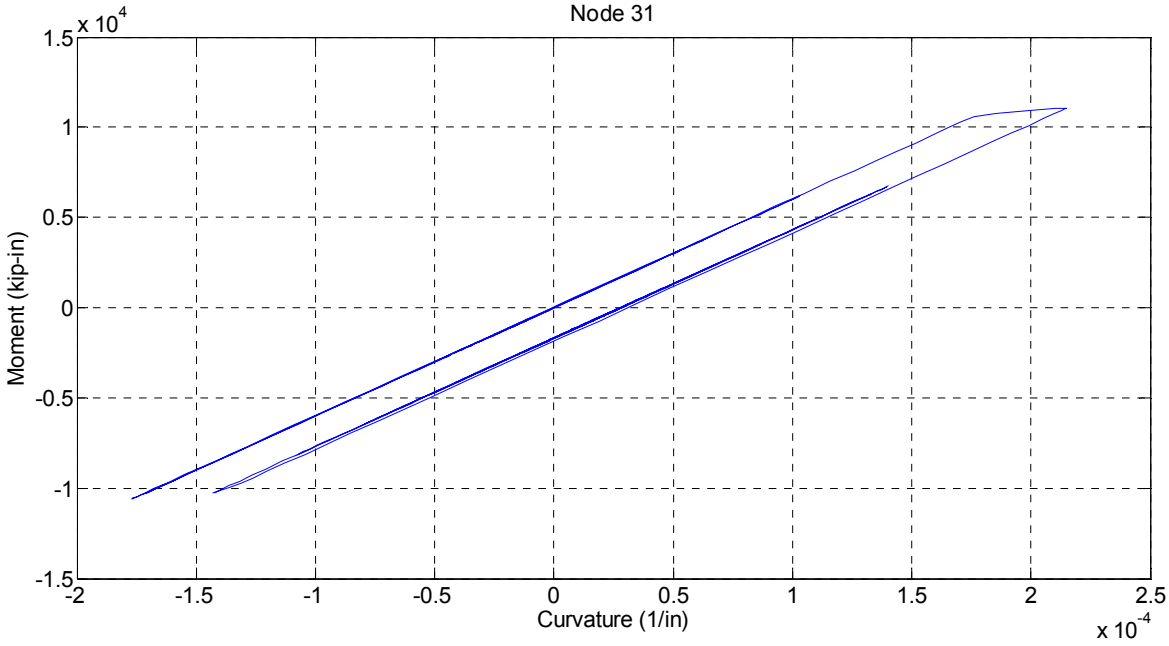

Figure 24: Moment Curvature Hysteresis Node 31

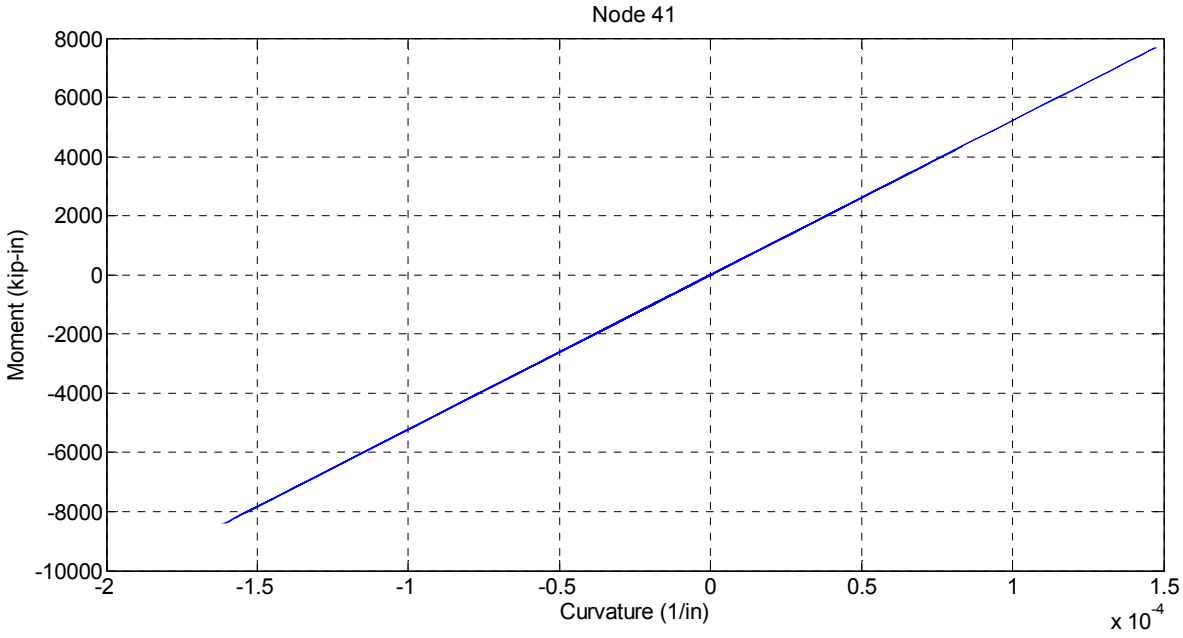

Figure 25: Moment Curvature Hysteresis Node 41

From the nonlinear inelastic analysis of the Elastic Frame model and the Condensed Hysteretic Model, it can clearly be verified that the Peak Displacements of the two models are the same. On checking the natural frequency of the first three modes, the values of the two models were identical. Hence, this is new method of Model Condensation using Hysteretic Parameters can be used to reduce the full model when performing any kind of seismic analysis.

5.5 Verification of condensed hysteretic model for inelastic dynamic response

The inelastic dynamic response of the condensed hysteretic model (with hysteretic parameters fit to a pulse response) was then verified with the high-fidelity model. The set of thirteen ATC – 63 near fault ground motion records containing a pulse were used to obtain a set of inelastic dynamic responses for both the condensed hysteretic model and the High Fidelity model. Table 6 represents the set of ground motions used with their respective magnify normalization factors to obtain inelastic behavior.

Table 6: The list of ground motions used, according to the NGA number with the high-pass frequency and low-pass frequency cut-off values, time step, and number of points.

Ground Motion Record	Inelastic Norm. factor	NPTS	HP	LP	DT
NGA 0181	2.7	7810	0.1	40	0.005
NGA 0182	1.92	7364	0.1	40	0.005
NGA 0292	3.44	16392	0.13	30	0.0024
NGA 0723	1.56	2235	0.06	20	0.01
NGA 0802	2.445	7991	0.1	38	0.005
NGA 0821	1.15	4262	0.1	40	0.005
NGA 0879	2.31	9625	0.08	60	0.005
NGA 1063	0.69	1991	0.06	30	0.01
NGA 1086	1.00	2000	0.12	23	0.02
NGA 1165	3.2	6000	0.1	30	0.005
NGA 1503	1.3	18000	0.03	50	0.005
NGA 1529	2.0	18000	0.04	50	0.005
NGA 1605	2.5	5177	0.06	50	0.005

The condensed hysteretic model was checked for the inelastic dynamic response (Horizontal floor displacements), the inter-story drift ratio and the relative floor acceleration for each of the given earthquake ground motions.

Table 7: Verification of the Hysteretic Model Condensation Method for Inelastic Structural behavior via comparison with a high fidelity model

Ground Motion used	Maximum Relative Floor Acceleration (g)		Maximum Inter-story Drift Ratio		Maximum Horizontal Displacement (in)	
	Full Model	Condensed Model	Full Model	Condensed Model	Full Model	Condensed Model
NGA 0181	1.5477	1.8735	0.0316	0.0323	16.3898	16.0708
NGA 0182	1.3300	1.2634	0.0295	0.0357	14.6876	15.9923
NGA 0292	2.0005	1.8777	0.0232	0.0229	11.8211	12.6104
NGA 0723	1.4854	1.4427	0.0281	0.0310	13.8503	14.6670
NGA 0802	1.8473	1.7650	0.0255	0.0303	14.2069	13.8720
NGA 0821	1.0341	0.9108	0.0211	0.0191	10.6621	10.8463
NGA 1063	1.5789	1.3366	0.0315	0.0341	15.7652	16.2719
NGA 1086	1.3945	1.3781	0.0232	0.0240	11.1283	11.3958
NGA 1165	1.2778	1.3063	0.0209	0.0194	10.7782	11.4332
NGA 1503	1.2617	1.2227	0.0298	0.0313	11.7887	11.3610
NGA 1529	1.2042	1.1205	0.0232	0.0247	11.6421	12.5038
NGA 1605	2.1801	2.2728	0.0287	0.0349	12.7172	11.6812

From table 7, it is evident that the condensed hysteretic model gives a very close approximation of the different seismic demands. The error is well within the acceptable range as in the field of earthquake engineering, earlier methods of such as the Modal Pushover Analysis and the Response Spectra Analysis both predict the seismic demands having errors much greater than the ones obtained from this new proposed model reduction method. Importantly, the condensed inelastic model is better at predicting inter-story drift ratios than peak floor displacements and peak floor accelerations. The

figures below show the Inelastic Earthquake Response (Horizontal floor displacements), Inter-story drift ratio and the relative floor acceleration of the High Fidelity OpenSees model and the condensed hysteretic model for two different earthquake ground motion (i.e. NGA 0181 and NGA 0292)

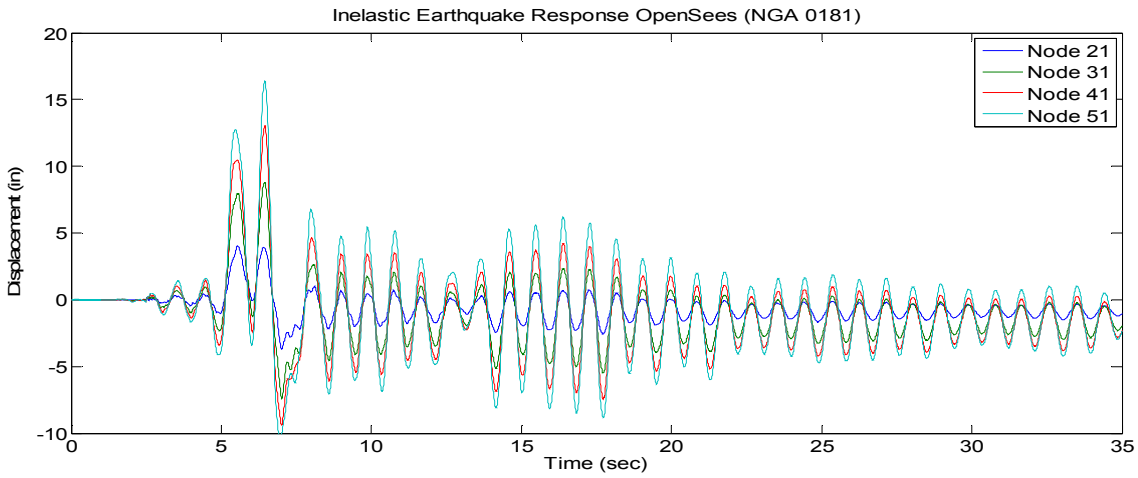

Figure 26: Inelastic Earthquake Response for the High Fidelity OpenSees model (NGA 0181)

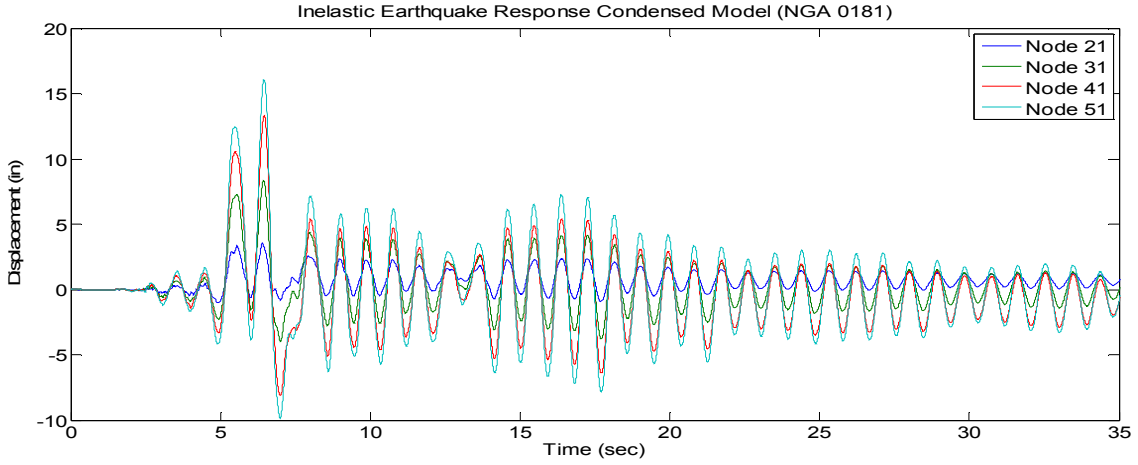

Figure 27: Inelastic Earthquake Response for the Condensed Hysteretic model (NGA 0181)

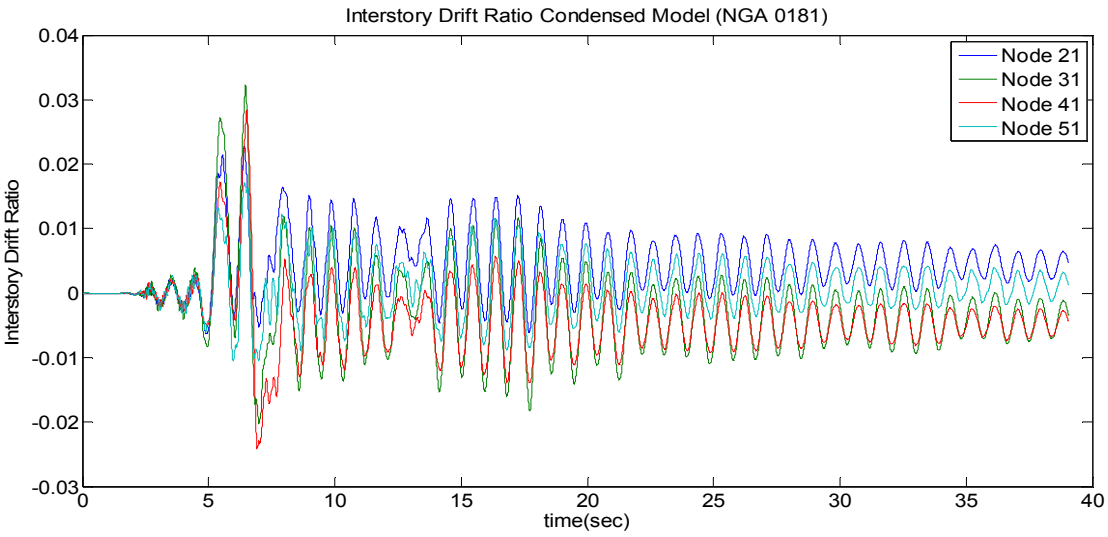

Figure 28: Inter-story Drift Ratio of the Condensed Hysteretic model (NGA 0181)

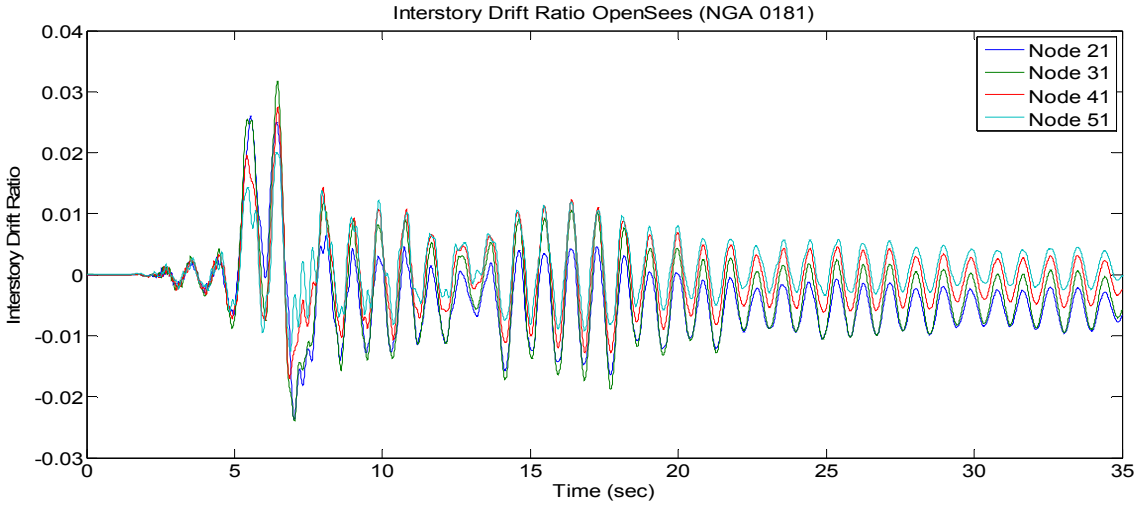

Figure 29: Inter-story Drift Ratio of the High-Fidelity OpenSees model (NGA 0181)

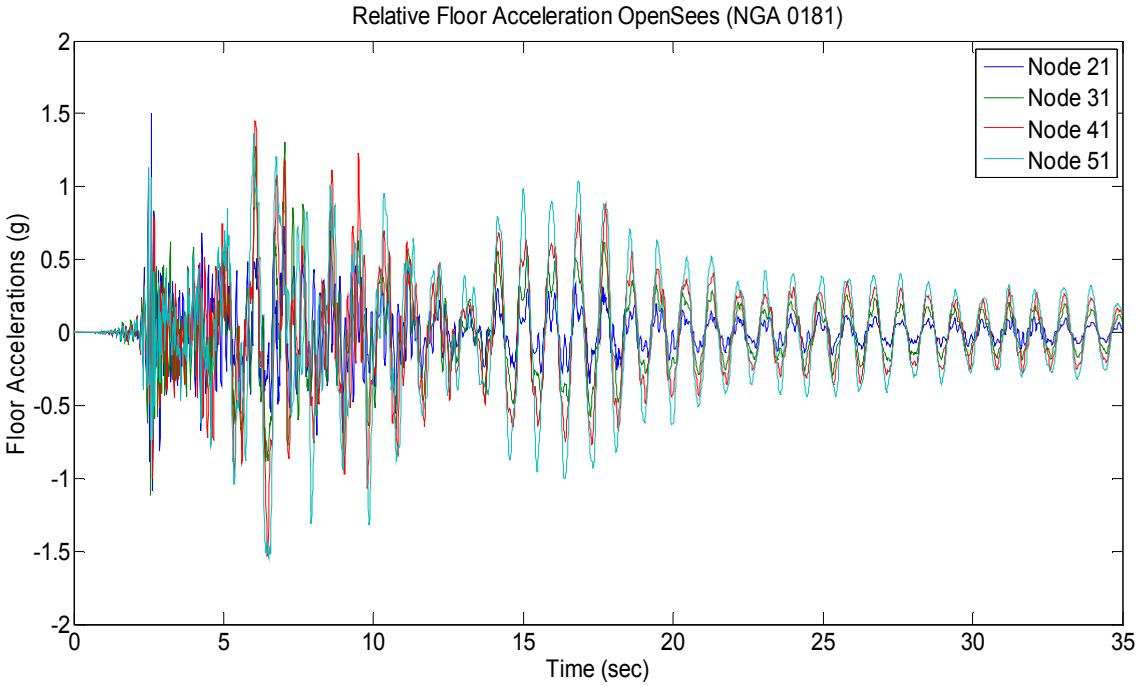

Figure 30: Relative Floor Acceleration High Fidelity model (NGA 0181)

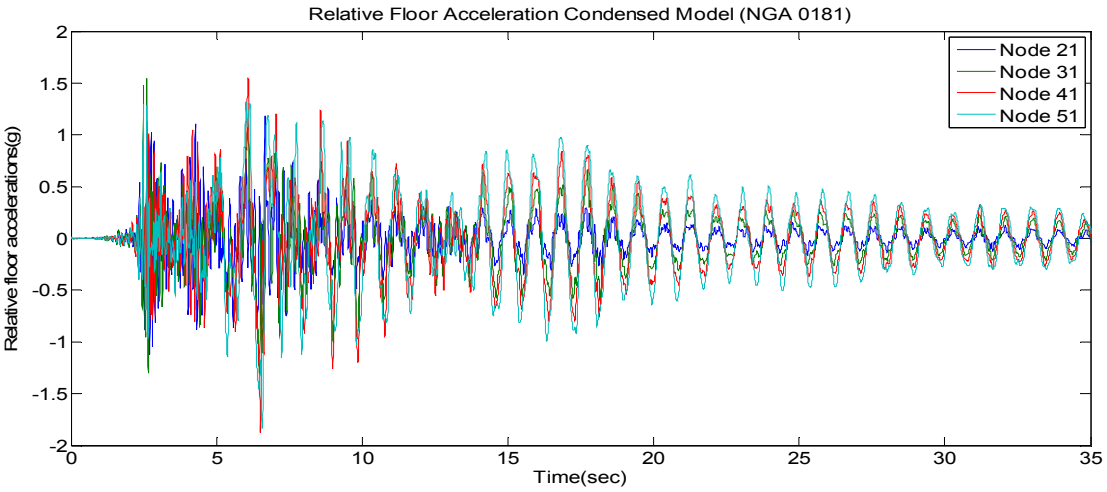

Figure 31: Relative Floor Acceleration Condensed Hysteretic Model (NGA 0181)

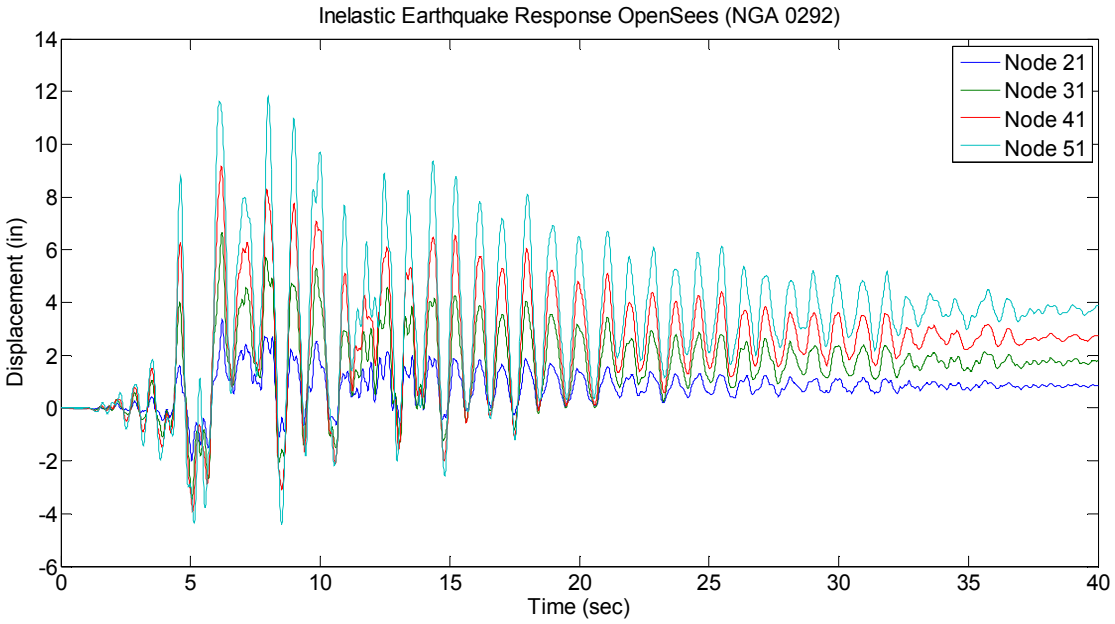

Figure 32: Inelastic Earthquake Response of the High Fidelity OpenSees Model (NGA 0292)

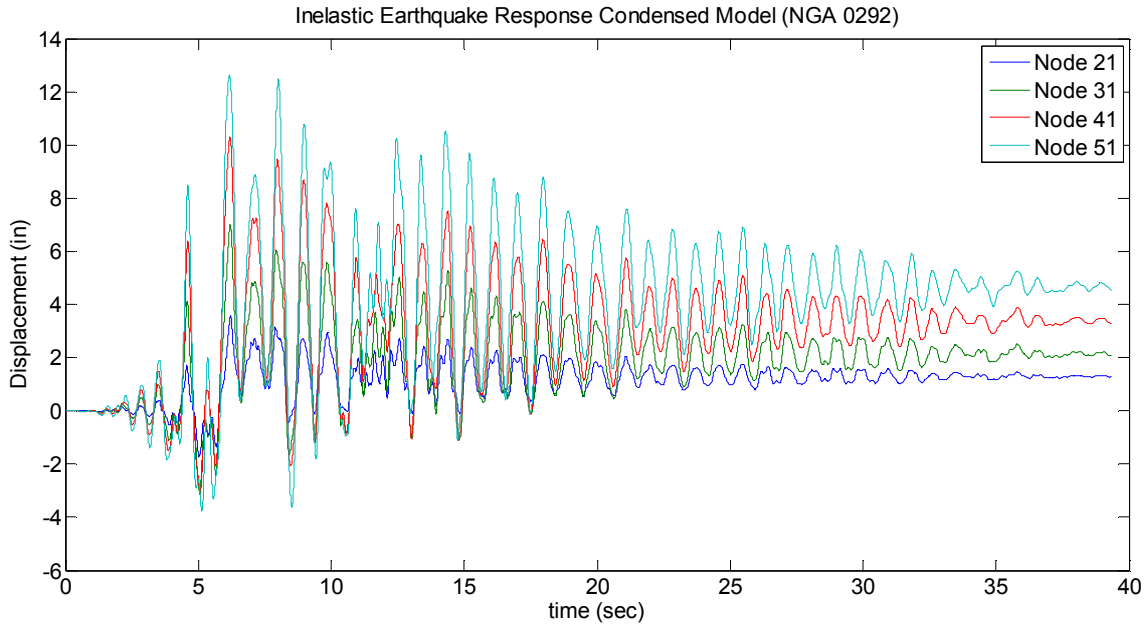

Figure 33: Inelastic Earthquake Response Condensed Hysteretic Model (NGA 0292)

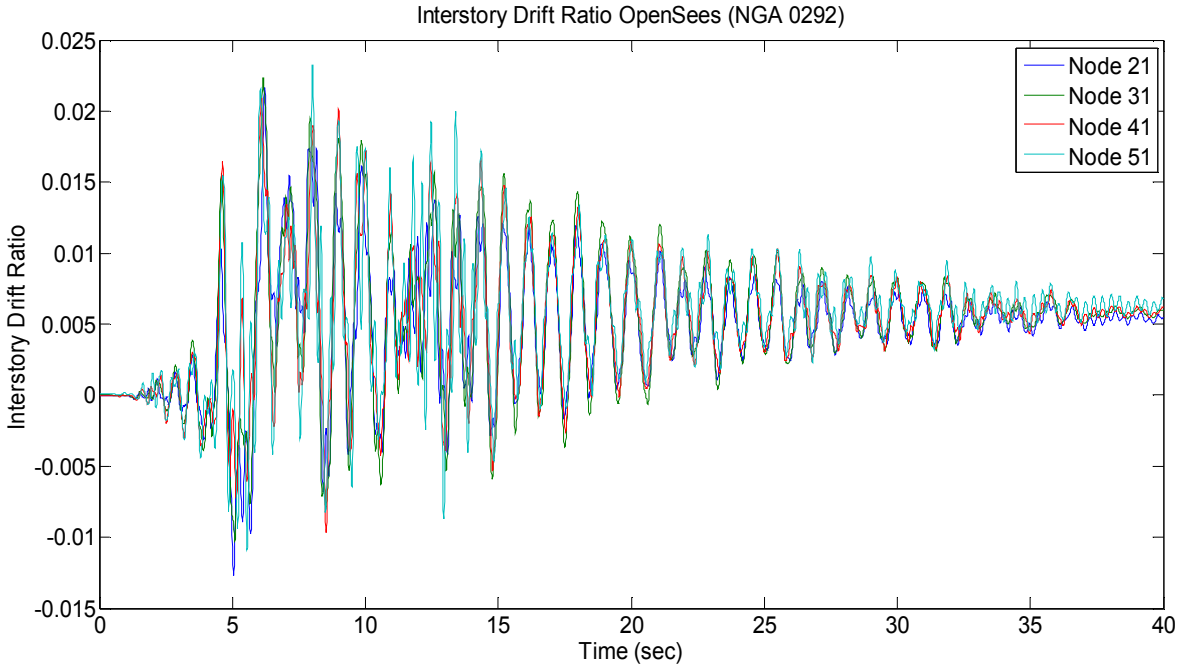

Figure 34: Inter-story Drift Ratio of the High Fidelity OpenSees model (NGA 0292)

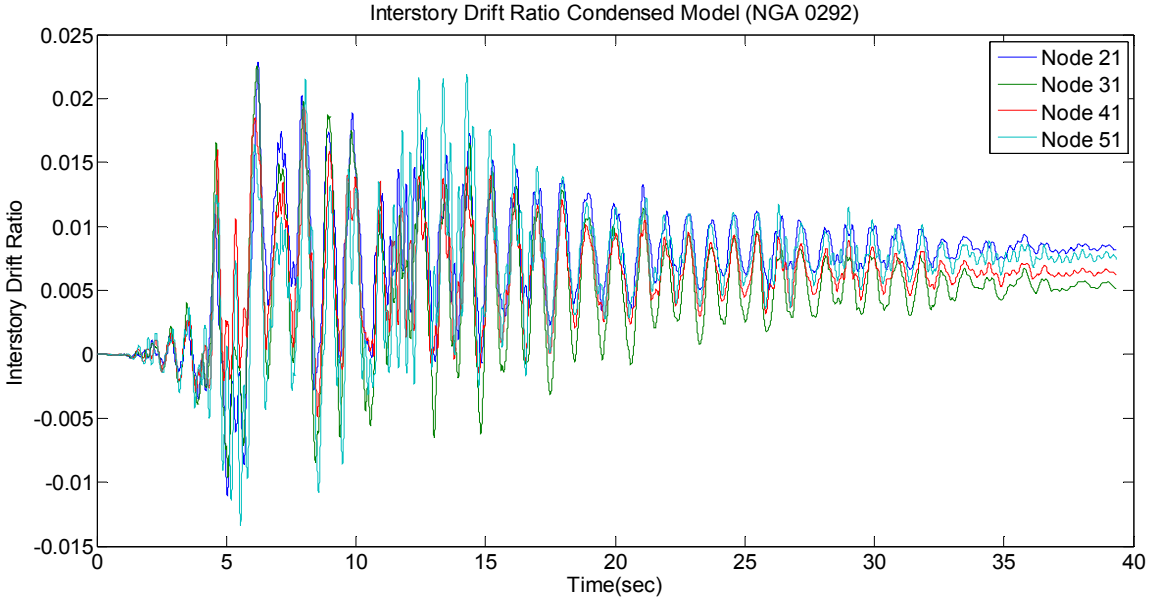

Figure 35: Inter-story Drift ratio of the Condensed Hysteretic model (NGA 0292)

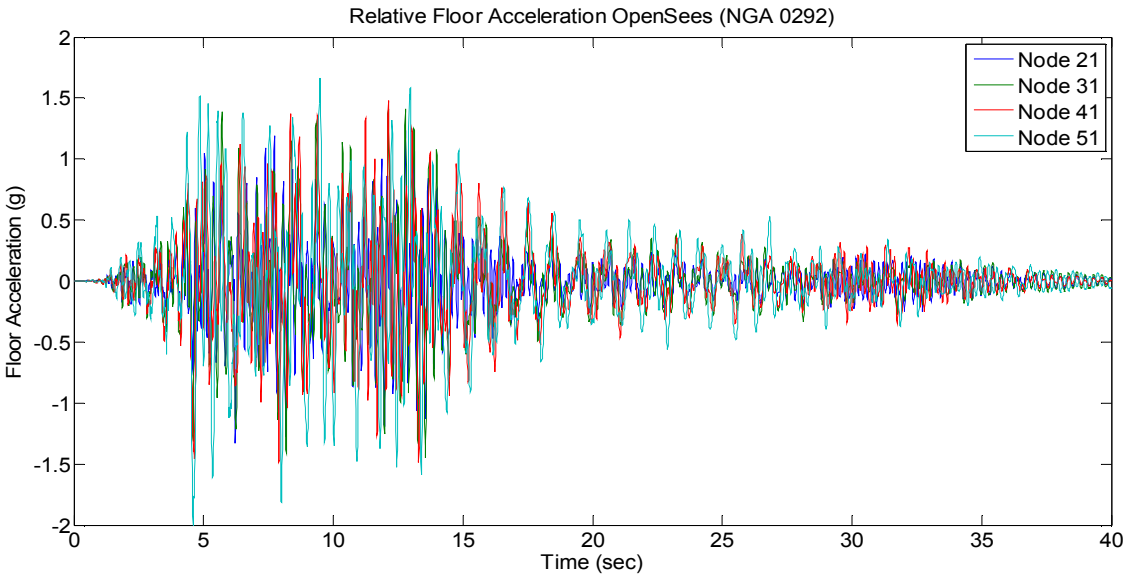

Figure 36: Relative Floor Acceleration of the High Fidelity OpenSees model (NGA 0292)

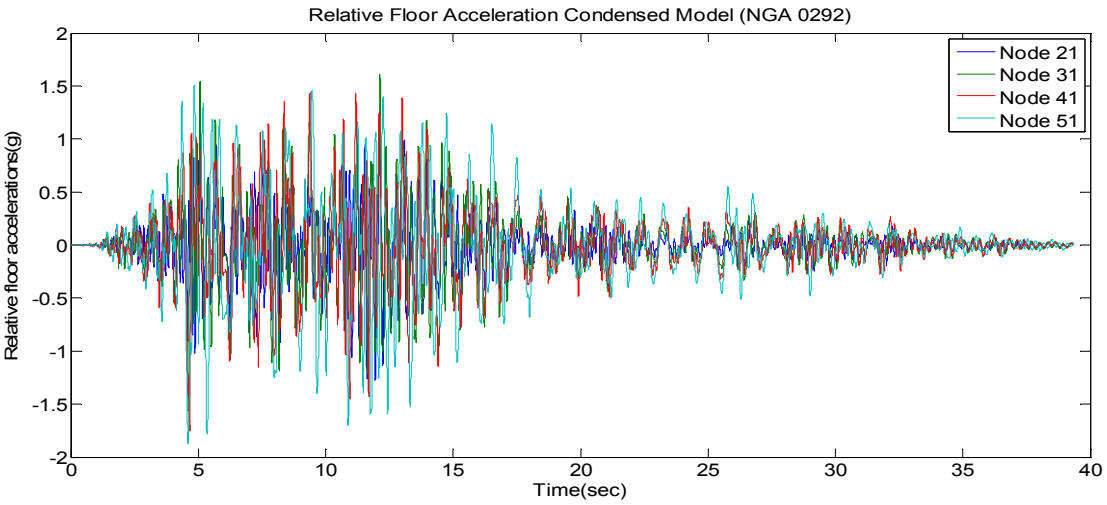

Figure 37: Relative Floor Acceleration of the Condensed Hysteretic Model (NGA 0292)

The error between the Condensed Hysteretic Model and the High Fidelity OpenSees model is given in Table 8 below.

Table 8: Relative Error between the condensed inelastic model and the high fidelity inelastic model for each of the earthquakes used in the model verification

Ground Motion Record	Error in Max. Horizontal Displacement	Error in Max. Inter-story Drift ratio	Error in Max. Relative Floor Acceleration
NGA 0181	1.94 %	2.21 %	21.05 %
NGA 0182	8.88 %	21.01 %	4.93 %
NGA 0292	6.67 %	1.29 %	6.13 %
NGA 0723	5.89 %	10.32 %	2.87 %
NGA 0802	2.35 %	18.82 %	4.45 %
NGA 0821	1.72 %	9.47 %	11.92 %
NGA 1063	3.21 %	8.25 %	15.34 %
NGA 1086	2.40 %	3.44 %	1.17 %
NGA 1165	6.07 %	7.17 %	2.23 %
NGA 1503	3.62 %	5.03 %	3.09 %
NGA 1529	7.40 %	6.46 %	6.95 %
NGA 1605	8.14 %	21.60 %	4.25 %

In an effort to improve the accuracy of the reduced hysteretic model, the response from the condensed model was fitted to a 5 second pulse response of the high fidelity model subjected to a high amplitude pulse of a period of 0.5 seconds. The new hysteretic parameters obtained were as follows:

$$\kappa = 0.0330$$

$$z_{yield} = [\, 1.6503; 2.1749; 1.8167; 1.7117 \,]$$

$$\eta = 6.2390$$

$$\rho = 0.5$$

These parameters were obtained by using $\rho = 0.5$ as a constant and by setting the maximum and minimum values as follows:

Table 9: Maximum and Minimum values used for the curve fitting process

Hysteretic Parameters	Maximum Value	Minimum Value
κ	0.2	0.02
z_{yield}	2.5	1.2
η	12.0	3.0

These hysteretic parameters obtained by curve fitting a 5 second high amplitude pulse response were then used to calculate the seismic demands with the reduced hysteretic model in order to check its accuracy. The following are the seismic demands calculated using the above parameters:

Table 10: Verification of the Hysteretic Model Condensation Method for Inelastic Structural behavior via comparison with a high fidelity model using the hysteretic parameters obtained by curve fitting for 5 seconds

Ground Motion Used	Maximum Horizontal Displacement		Maximum Inter-story Drift Ratio		Maximum Floor Acceleration	
	OpenSees	Matlab	OpenSees	Matlab	OpenSees	Matlab
NGA 0181	16.3898	15.4577	0.0316	0.0317	1.5477	1.8051
NGA 0182	14.6876	15.6971	0.0295	0.0321	1.3300	1.2306
NGA 0292	11.8211	12.2528	0.0232	0.0229	2.0005	1.8362
NGA 0723	13.8503	14.0209	0.0281	0.0282	1.4854	1.3890
NGA 0802	14.2069	13.9767	0.0255	0.0302	1.8473	1.6938
NGA 0821	10.6621	11.0354	0.0211	0.0200	1.0341	0.8517
NGA 0879	8.9792	10.0147	0.0175	0.0246	2.3454	2.8124
NGA 1063	15.7652	16.2346	0.0315	0.0328	1.5789	1.3204
NGA 1086	11.1283	10.9918	0.0232	0.0226	1.3945	1.3778
NGA 1165	10.7782	11.2476	0.0209	0.0204	1.2778	1.2994
NGA 1503	11.7887	11.4751	0.0298	0.0284	1.2617	1.1238
NGA 1529	11.6421	11.2742	0.0232	0.0229	1.2042	0.9892
NGA 1605	12.7172	11.6154	0.0287	0.0338	2.1801	2.2380

Table 11: The error between the High Fidelity OpenSees model and the Condensed hysteretic Matlab model using the hysteretic parameters obtained by curve fitting the 5 second response

Ground Motion	Error in Max. Horizontal Displacement (%)	Error in Max. Inter-story Drift Ratio (%)	Error in Max. Floor Acceleration (%)
NGA 0181	5.687	0.316	16.631
NGA 0182	6.873	8.813	7.473
NGA 0292	3.652	1.293	8.213
NGA 0723	1.232	0.355	6.489
NGA 0802	1.620	18.431	8.309
NGA 0821	3.501	5.213	17.638
NGA 0879	11.532	28.861	19.911
NGA 1063	2.977	4.127	16.372
NGA 1086	1.226	2.586	1.197
NGA 1165	4.355	2.392	1.690
NGA 1503	2.660	4.678	10.929
NGA 1529	3.160	1.293	17.854
NGA 1605	8.664	17.770	2.655
Average Error	4.396	7.394	10.412

To further improve the response, the response from the condensed model was fitted to a 2 second pulse response of the High Fidelity OpenSees model subjected to a high Amplitude Pulse of a period of 0.5 seconds. The new hysteretic parameters obtained were as follows:

$$\kappa = 0.1167$$

$$z_{yield} = [\ 1.5388; 2.0619; 1.7145; 1.6115\ ]$$

$$\eta = 8.1826$$

$$\rho = 0.5$$

These parameters were obtained by using $\rho = 0.5$ as a constant and by setting the maximum and minimum values as follows:

Table 12: Maximum and Minimum values used for the curve fitting for a 2 second response

Hysteretic Parameters	Maximum Value	Minimum Value
κ	0.2	0.02
z_{yield}	2.5	1.2
η	12.0	3.0

The following are the seismic demands calculated using the hysteretic parameters obtained by curve fitting the 2 second high amplitude pulse response.

Table 13: Verification of the Hysteretic Model Condensation Method for Inelastic Structural behavior via comparison with a high fidelity model using the hysteretic parameters obtained by curve fitting for 2 seconds

Ground Motion Used	Maximum Horizontal Displacement		Maximum Inter-story Drift Ratio		Maximum Floor Acceleration	
	OpenSees	Matlab	OpenSees	Matlab	OpenSees	Matlab
NGA 0181	16.3898	14.7276	0.0316	0.0288	1.5477	1.7904
NGA 0182	14.6876	14.3817	0.0295	0.0280	1.3300	1.2445
NGA 0292	11.8211	12.4680	0.0232	0.0225	2.0005	1.8261
NGA 0723	13.8503	13.7278	0.0281	0.0286	1.4854	1.4083
NGA 0802	14.2069	14.1546	0.0255	0.0279	1.8473	1.8523
NGA 0821	10.6621	11.0535	0.0211	0.0201	1.0341	0.8365
NGA 0879	8.9792	10.2520	0.0175	0.0236	2.3454	2.8049
NGA 1063	15.7652	16.2732	0.0315	0.0336	1.5789	1.3212
NGA 1086	11.1283	11.0019	0.0232	0.0224	1.3945	1.3305
NGA 1165	10.7782	11.2117	0.0209	0.0194	1.2778	1.3453
NGA 1503	11.7887	10.9567	0.0298	0.0253	1.2617	1.0494
NGA 1529	11.6421	10.7151	0.0232	0.0217	1.2042	0.9825
NGA 1605	12.7172	11.6544	0.0287	0.0292	2.1801	2.5159

The error between the High Fidelity OpenSees model and the Condensed hysteretic Matlab model were then calculated:

Table 14: The error between the High Fidelity OpenSees model and the Condensed hysteretic Matlab model using the hysteretic parameters obtained by curve fitting the 2 second response

Ground Motion	Error in Max. Horizontal Displacement (%)	Error in Max. Inter-story Drift Ratio (%)	Error in Max. Floor Acceleration (%)
NGA 0181	10.141	8.861	15.681
NGA 0182	2.082	5.084	6.428
NGA 0292	5.472	3.017	8.942
NGA 0723	0.884	1.779	5.190
NGA 0802	0.368	9.411	0.271
NGA 0821	3.671	4.739	19.108
NGA 0879	14.175	34.857	19.591
NGA 1063	3.222	6.667	16.321
NGA 1086	1.135	3.448	4.589
NGA 1165	4.022	7.177	5.282
NGA 1503	7.057	15.100	16.826
NGA 1529	7.962	6.465	18.410
NGA 1605	8.537	1.742	15.403
Average Error	5.286	8.336	11.695

Since the average error has increased, the hysteretic parameters were again calculated by fitting the response from the condensed model to a 5 second pulse response of the High Fidelity OpenSees model subjected to a high Amplitude Pulse of a period of 0.5 seconds. But this time the number of hysteretic parameters was increased. Instead of using a constant value for the hysteretic shape factor (ρ), the value of obtained by curve fitting. The new hysteretic parameters obtained were as follows:

$$\kappa = 0.1206$$

$$z_{yield} = [\ 1.562; 2.054; 1.672; 1.532\ ]$$

$$\eta = 12.000$$

$$\rho = [\ 1.000; 0.711; 0.1; 0.1\ ]$$

Table 15: Maximum and Minimum values used for the curve fitting for a 5 second response with varying hysteretic shape factor

Hysteretic Parameters	Maximum Value	Minimum Value
κ	0.2	0.02
z_{yield}	2.5	1.2
η	12.0	3.0
ρ	1.0	0.1

Table 16: Verification of the Hysteretic Model Condensation Method for Inelastic Structural behavior via comparison with a high fidelity model using the hysteretic parameters obtained by curve fitting for 5 seconds with varying hysteretic shape factor

Ground Motion Used	Maximum Horizontal Displacement		Maximum Inter-story Drift Ratio		Maximum Floor Acceleration	
	OpenSees	Matlab	OpenSees	Matlab	OpenSees	Matlab
NGA 0181	16.3898	15.2651	0.0316	0.0311	1.5477	1.9793
NGA 0182	14.6876	14.4300	0.0295	0.0285	1.3300	1.3638
NGA 0292	11.8211	12.6583	0.0232	0.0256	2.0005	1.8056
NGA 0723	13.8503	14.1169	0.0281	0.0277	1.4854	1.5515
NGA 0802	14.2069	14.5338	0.0255	0.0286	1.8473	2.2986
NGA 0821	10.6621	11.2427	0.0211	0.0199	1.0341	0.9493
NGA 0879	8.9792	9.5076	0.0175	0.0214	2.3454	2.8354
NGA 1063	15.7652	16.7259	0.0315	0.0329	1.5789	1.3512
NGA 1086	11.1283	11.7101	0.0232	0.0223	1.3945	1.3437
NGA 1165	10.7782	11.1807	0.0209	0.0192	1.2778	1.4081
NGA 1503	11.7887	10.8506	0.0298	0.0280	1.2617	1.1576
NGA 1529	11.6421	11.4687	0.0232	0.0230	1.2042	1.1299
NGA 1605	12.7172	11.6229	0.0287	0.0322	2.1801	2.4240

The error between the High Fidelity OpenSees model and the Condensed hysteretic Matlab model were then calculated:

Table 17: The error between the High Fidelity OpenSees model and the Condensed hysteretic Matlab model using the hysteretic parameters obtained by curve fitting the 5 second response with varying hysteretic shape factor

Ground Motion	Error in Max. Horizontal Displacement (%)	Error in Max. Inter-story Drift Ratio (%)	Error in Max. Floor Acceleration (%)
NGA 0181	6.862	1.582	27.886
NGA 0182	1.754	3.389	2.54
NGA 0292	7.082	10.344	9.742
NGA 0723	1.925	1.423	4.449
NGA 0802	2.301	12.156	24.412
NGA 0821	5.445	5.687	8.200
NGA 0879	5.884	22.285	20.853
NGA 1063	6.094	4.444	14.421
NGA 1086	5.228	3.879	3.642
NGA 1165	3.734	8.134	10.197
NGA 1503	7.957	6.040	8.250
NGA 1529	1.489	0.862	6.17
NGA 1605	8.604	12.195	11.187
Average Error	4.950	7.109	11.688

The Average Errors in seismic demands for different parameters were then examined in order to find the most appropriate way to calculate the hysteretic parameters. The table below represents the average error between the High Fidelity OpenSees model and Condensed hysteretic model for the different hysteretic parameters used by curve fitting the high amplitude pulse for different response periods and number of parameters:

Table 18: Average Error for different seismic demands for the different hysteretic parameters used

	Maximum Horizontal Displacement (%)	Maximum Inter-Story Drift Ratio (%)	Maximum Floor Acceleration (%)
Hysteretic Parameters obtained by fitting 17.5 second response	4.960	11.761	7.390
Hysteretic Parameters obtained by fitting 5 second response	4.396	7.394	10.412
Hysteretic Parameters obtained by fitting 2 second response	5.286	8.336	11.685
Hysteretic Parameters obtained by fitting 5 second response with varying ρ	4.950	7.109	11.688

From the table, it can be observed that the hysteretic parameters obtained by fitting the 5 second response with varying hysteretic shape factor gives the most accurate result in terms of the Maximum Inter-story Drift ratio. Whereas, by using a constant hysteretic shape factor of 0.5, the hysteretic parameters obtained by fitting the 5 second pulse response give the most accurate Maximum Horizontal Displacement and Maximum Floor Acceleration. In both the cases, it is clear that the hysteretic parameters obtained by fitting the 5 second high amplitude pulse response which shows the first 2

cycles give the most accurate seismic demands when compared with the High Fidelity OpenSees model.

6. Conclusions

From the above observations, it is clear that the proposed model reduction method has an error rate that is acceptable by the profession. The reason for this error lies in the approximation in the hysteretic parameters. Since, the curve fitting did not completely converge at a high tolerance, approximate values were used throughout the inelastic dynamic analysis.

Further study in the approximation of the hysteretic parameters can reduce this error. The number of hysteretic parameters used in this case was 7, which can be increased to 13. This can have an effect on the reduction of the error in the seismic demands between the detailed model and the condensed hysteretic model.

Since, the hysteretic parameters were obtained as an approximation by curve fitting the high amplitude pulse response of the detailed model and the condensed model, there can be other ways of obtaining these hysteretic parameters. This too can bring down the error in the seismic demands of the condensed hysteretic model and the detailed model.

Finally, by applying this method of model reduction, the total number of degrees of freedom was reduced from 60 to 4. A 3D analysis using the proposed method should be carried out as the reduction in the total number of degrees of freedom will be extremely high, thus, reducing computational cost.

References

[1] Building Seismic Safety Council. NEHRP Guidelines for the Seismic Rehabilitation of Buildings, FEMA 273, Washington, DC, 1997.

[2] Response History Analysis, Dynamics of Structures by Anil K. Chopra, Chapter 13.1

[2] Saiidi M, Sozen MA. Simple non-linear seismic analysis of RC structures, *Journal of Structural Division,* ASCE 1981

[3] Structural Dynamics by Mario Paz, Chapter 13.1, 1985

[4] Structural Dynamics by Mario Paz, Chapter 13.4, 1985

[5] Robert J. Guyan Reduction of Stiffness and Mass Matrixes, AIAA Journal Vol 3, No.2

[6] M. Paz Dynamic Condensation, AIAA Journal 22 (1985) 724 - 727

[7] Anil K. Chopra & Rakesh K. Goel , A Modal Pushover Analysis procedure for estimating seismic demands for buildings, Earthquake Engineering and Structural Dynamics 2002; 31:561-582

[8] Chopra A.K. Dynamics of Structures: Theory and Applications to Earthquake Engineering. Prentice-Hall: Englewood Cliffs, NJ, 2001.

[9] Wilson, E. L., Suharwardy, I., & Habibullah, A. (1995). A Clarification of the Orthogonal Effects in a Three-Dimensional Seismic Analysis. *Earthquake Spectra, 11*, 659-666.

[9] Y. J. Park, Y. K. Wen, A. H.-S. Ang, Random vibration of hysteretic systems under bi-directional ground motion, Earthquake Engineering and Structural Dynamics 14 (1986) 543–557.

[10] R. Bouc, Forced vibration of mechanical systems with hysteresis, in: Proceedings of the Fourth Conference on Nonlinear Oscillation, Prague, Czechoslovakia, 1967.

[11] Y.-K. Wen, Method for random vibration of hysteretic systems, Journal of Engineering Mechanics 102 (1976) 249–263.

[12] Silvia Mazzoni, Frank McKenna, Michael H. Scott, Gregory L. Fenves, et al. OpenSees Command Language Manual

[13] Henri P. Gavin, The Levenberg-Marquardt method for nonlinear least squares curve-fitting problems

[14] P. Scott Harvey, Jr. and Henri P. Gavin," Truly Isotropic Biaxial Hysteresis with Arbitrary Knee Sharpness" EARTHQUAKE ENGINEERING AND STRUCTURAL DYNAMICS Earthquake Engineering Structural Dynamics 2013;

[15] C. W. Wong, Y. Q. Ni, J. M. Ko, Stead-state oscillation of hysteretic differential model II: Performance analysis, Journal of Engineering Mechanics 120 (11) (1994) 2299–2325. doi:10.1061/(ASCE)0733-9399(1994)120:11(2271).

[16] K. Levenberg. "A Method for the Solution of Certain Non-Linear Problems in Least Squares". The Quarterly of Applied Mathematics, 2: 164-168 (1944).

[17] M.I.A. Lourakis. A brief description of the Levenberg-Marquardt algorithm implemented by levmar, Technical Report, Institute of Computer Science, Foundation for Research and Technology - Hellas, 2005.

[18] K. Madsen, N.B. Nielsen, and O. Tingleff. Methods for nonlinear least squares problems. Technical Report. Informatics and Mathematical Modeling, Technical University of Denmark, 2004.

[19] D.W. Marquardt. "An algorithm for least-squares estimation of nonlinear parameters," Journal of the Society for Industrial and Applied Mathematics, 11(2):431-441, 1963.

[20] H.B. Nielson, Damping Parameter In Marquardt's Method, Technical Report IMM-REP-1999- 05, Dept. of Mathematical Modeling, Technical University Denmark.

[21] W.H. Press, S.A. Teukosky, W.T. Vetterling, and B.P. Flannery. Numerical Recipes in C, Cambridge University Press, second edition, 1992.

[22] Mark K.Transtrum, Benjamin B. Machta, and James P. Sethna, "Why are nonlinear fits the data so challenging?", Phys. Rev. Lett. 104, 060201 (2010),

[23] Mark K. Transtrum and James P. Sethna "Improvements to the Levenberg-Marquardt algorithm for nonlinear least-squares minimization," Preprint submitted to Journal of Computational Physics, January 30, 2012.

[24] PEER Ground motion database http://peer.berkeley.edu/smcat/data.html

[25] Applied Technology Council, Quantification of building seismic performance factors. URL https://www.atcouncil.org/Projects/atc-63-project.html

[26] EPFrame, nees.org URL https://nees.org/tools/epframe/wiki

[27] F.T. Mckenna, Object-Oriented Finite Element Programming: Frameworks for Analysis, Algorithms & Parallel Computing (1997)

[28] R.M. De Souza, Force-based Finite Element for Large Displacement Inelastic Analysis of Frames (2000)

[29] H. Krawinkler, G. Seneviratna, Pros and Cons of a push over analysis of seismic performance evaluation (1998), *Engineering Structures 1998, Elsevier*